Behavior of an MHD generator operating around the critical point
by Conwell James Dickey

A thesis submitted in partial fulfillment of the requirements for the degree of MASTER OF SCIENCE in Electrical Engineering
Montana State University

Abstract:
The defining equations for MHD flow were presented. A numerical means of approximate solution of these equations was developed.

A summary of the current theory of steady, state MHD flow and its consequences with regard to choking was then given. A study of transient, choked MHD flow was then presented, using the previously developed numerical model, and a comparison of steady and transient flow was given. Finally, a possible means of inferring the internal state of an MHD generator, based on terminal characteristics, was introduced.

STATEMENT OF PERMISSION TO COPY

In presenting this thesis in partial fulfillment of the requirements for an advanced degree at Montana State University, I agree that the Library shall make it freely available for inspection. I further agree that permission for extensive copying of this thesis for scholarly purposes may be granted by my major professor, or in his absence, by the Director of Libraries. It is understood that any copying or publication on this thesis for financial gain shall not be allowed without my written permission.

Signature Conwell Dickey

Date Oct. 27, 1975

103

BEHAVIOR OF AN MHD GENERATOR
OPERATING AROUND THE CRITICAL POINT

by

CONWELL JAMES DICKEY

A thesis submitted in partial fulfillment
of the requirements for the degree

of

MASTER OF SCIENCE

in

Electrical Engineering

Approved:

R. M. Johnson
Chairman, Examining Committee

Paul E. Uhlrich
Head, Major Department

Henry L. Parsons
Graduate Dean

MONTANA STATE UNIVERSITY
Bozeman, Montana

October, 1975

ACKNOWLEDGEMENTS

The author wishes to sincerely thank his advisor, Dr. Roy M. Johnson, for his encouragement and guidance in the development of this research. The helpful suggestions of Dr. Robert F. Durnford and Dr. Donald A. Pierre were also greatly appreciated.

Finally, the author would like to offer a special thanks to his mother, Virginia, for her encouragement during his pursuit of his education, and to his wife, Vivian, for her patience and encouragement during the course of this research.

TABLE OF CONTENTS

LIST OF TABLES

LIST OF FIGURES

LIST OF SYMBOLS

Symbol		Page First Encountered
a	speed of sound, meters/second	2
A	channel cross-sectional area, square meters	14
$\underline{B}$	magnetic flux density, webers/square meter	7
B, B_z	z-component of magnetic flux density, wb/sq m	10
C	Duct circumference, meters	14
c	characteristic speed, meter/second	21
C_f	friction factor	14
C_p	specific heat at constant pressure	15
C_v	specific heat at constant volume	16
$\underline{E}$	Electric field, volts/meter	7
e	specific internal energy, N/m^2s	8
$\underline{E}'$	rest frame electric field, volts/meter	8
E_s	stagnation internal energy, N·m/kg·s	13
E_x	x-component of electric field, volts/ meter	68
E_y	y-component of electric field, volts/ meter	68
E_z	z-component of electric field, volts/ meter	68
F	friction force per unit volume, N/sq m	12
$\underline{F}(\underline{U})$	three element vector	18
$\underline{G}(\underline{U})$	three element vector	18
$\underline{G}^*(\underline{U})$	three element vector	23
$\underline{H}(\underline{U})$	three element vector	23

Symbol		Page First Encountered
h	electrode walls separation, meters	11
I	current, amperes	54
$\underline{i}$	unit vector in x-direction	7
$\underline{J}$	current density, amperes/square meter	7
$\underline{J}'$	rest frame current density, amperes/ square meter	8
$\underline{j}$	unit vector in y-direction	7
J_x	x-component of current density, amperes/ square meter	68
J_y	y-component of current density, amperes/ square meter	68
J_z	z-component of current density, amperes/ square meter	68
JP	a ratio	59
$(\underline{J}x\underline{B})_x$	x-component of $\underline{J}x\underline{B}$, newtons/ cubic meter	13
K	loading factor or parameter	14
$\underline{k}$	unit vector in z-direction	7
L	channel length, meters	11
ℓ	insulator walls separation, meters	14
M	Mach number	2
m	momentum density, kg/ square meters·seconds	13
N_{st}	Stanton number	15
P	pressure, newtons/ square meter	7
P_e	exit pressure, newtons/ square meter	26
P_i	inlet pressure, newtons/ square meter	57
P_o	stagnation pressure, newtons/ square meter	26

Symbol		Page First Encountered
P^*	critical pressure, newtons/ square meter	27
Q	heat loss per unit volume	12
q_w	heat transfer to the walls, Joules/ meter·second	71
R	ideal gas constant, N·m/mole·$^{\circ}$K	8
Re	Reynolds number	14
R_i	internal resistance, Ohms	72
R_L	load resistance, Ohms	14
r_{cp}	critical pressure ratio	28
r_o	operating pressure ratio	28
T	temperature, $^{\circ}$Kelvin	8
T_e	exit temperature, $^{\circ}$Kelvin	27
T_o	stagnation temperature, $^{\circ}$Kelvin	27
T_w	wall temperature, $^{\circ}$Kelvin	15
t	time, seconds	6
$\underline{U}$	three element vector	18
u	x-component of velocity, meter/ second	2
u_e	exit velocity, meters/ second	27
V	voltage, volts	54
$\underline{V}$	vector velocity, meters/ second	6
v	y-component of velocity, meters/ second	7
v_{oc}	open-circuit voltage, volts	73
w	z-component of velocity, meters/ second	7

Symbol		Page First Encountered
α	percent of ionization	8
β	Hall parameter	68
γ	specific heat ratio	16
Δt	differential time step	19
Δx	differential x step	14
η	viscosity, poise	14
κ_T	thermal conductivity, Joules$\cdot{}^{o}$K/second$\cdot$meter	8
μ	mobility	68
$\bar{\mu}_o$	mean molecular weight, kg/mole	8
ρ	mass density, kg/cubic meter	6
ρ_e	charge density, Coulombs/cubic meter	7
σ	conductivity, mhos/meter	9
$\underleftrightarrow{\tau}'$	shear stress	7
τ_w	shear stress at wall	14
Φ	mechanical dissipation function	8
Ψ	gravitational potential	7

ABSTRACT

The defining equations for MHD flow were presented. A numerical means of approximate solution of these equations was developed. A summary of the current theory of steady state MHD flow and its consequences with regard to choking was then given. A study of transient, choked MHD flow was then presented, using the previously developed numerical model, and a comparison of steady and transient flow was given. Finally, a possible means of inferring the internal state of an MHD generator, based on terminal characteristics, was introduced.

CHAPTER I

1.1 Introduction

Magnetohydrodynamics (MHD), as a method of energy conversion, has recently been receiving much attention due to several attractive features. MHD offers a complete lack of moving parts in the generator as well as direct thermal to electrical energy conversion and, if the MHD generator is coupled with a steam bottoming plant, efficiencies approaching 60 percent are predicted for first generation systems. These features, as well as others, are sufficient reason to continue research leading toward the eventual development of MHD as a usable means of energy conversion.

The theory behind MHD has been available since the time of Faraday, when he stated his well-known principle of magnetic induction. This principle, stated simply, says that if a conductor is moved through a magnetic field, then a current will be induced in the conductor, such that its direction of flow is perpendicular to both the direction of movement of the conductor and the direction of the magnetic field. In the case of MHD, the conductor is a fluid which is heated to such a degree that it becomes a conductor through ionization. The fluid is then forced down a duct such that the direction of flow is perpendicular to an applied magnetic field. Then, by appropriate placement of pairs of electrodes on the duct walls, electrical energy can be extracted. This description of the MHD energy conversion process is an oversimplification but will suffice until the problem is more rigorously formulated in Chapter II. For the reader who is interested in the auxilary components necessary to operate an MHD facility, Rosa (1968) is an excellent source for introductory study.

When the governing equations for an MHD generator are developed in Chapter II, it will be seen that the equations exhibit an interesting characteristic. When the fluid velocity exceeds the local speed of sound (i.e., the flow is supersonic), the equations are hyperbolic, while if the fluid velocity is less than the local speed of sound (i.e., the flow is subsonic), the equations are elliptic (Hughes, 1966). This change of form would seem to indicate that any flow which is transonic might exhibit special behavior at the sonic point. This is indeed the case, and will be more rigorously defended later. To simplify the discussion, it is usual to define a Mach number, M, as

$$M = u/a \tag{1.1}$$

where u is the fluid velocity and a is the local speed of sound. Then for subsonic flow, M is less than one, and for supersonic flow, M is greater than one.

To understand the special behavior of the MHD flow at M = 1, it is necessary to understand the significance of the speed of sound. Sound propagates as pressure disturbances and the sonic speed is actually the speed of propagation of these pressure disturbances.

For a fluid with some given velocity, the velocity with which a pressure disturbance will propagate upstream is given by

$$a - u \qquad 1.2$$

If $u < a$, $(M < 1)$, then (1.2) assumes a positive value, and pressure disturbances are able to affect the flow upstream of their occurrence. However, if $u \geq a$, $(M \geq 1)$, (1.2) assumes a nonpositive value and pressure disturbances are unable to affect the upstream flow conditions. With this in mind, it is obvious why flow for $M = 1$ exhibits such special behavior. In fact, the behavior is so special that the $M = 1$ state is usually called the critical state, and in the absences of special conditions (usually the absence of a throat at the critical point), the flow is said to be choked when it reaches its critical point. The critical point has yet another significant property, however, in that it is the axis of mirror symmetry for the flow properties. That is to say, for a given MHD channel configuration, the flow of $M < 1$ will have a mirror symmetry with the flow for $M > 1$. For instance, a subsonic diffuser will act as a nozzle for supersonic flow. This is discussed in much more depth by Shapiro (1953). Deeper study into this symmetry will show, in fact, that a generator designed to be operated with subsonic (supersonic) flow will not operate properly with supersonic (subsonic) flow. Because of this, and the mirror symmetry, it is imperative that the critical state be avoided at all points in the channel if at all possible. Based on the preceeding discussion, we are now able to define the problem which this thesis will attempt to examine.

Since it is desirable to avoid choking in the generator, this thesis will attempt to relate the terminal characteristics of an MHD generator to the internal state of the generator, such that choking can either be avoided or, predicted to allow for compensation. To accomplish this, the work will be done in the following stages.

In Chapter II, a model which reasonably predicts the steady-state and transient response of an MHD generator will be developed. This model will then be used to develop an understanding of the generator under varied operating conditions. In Chapter III, an understanding of choking based on the principles of steady, one-dimensional compressible flow will be developed. This will also include a study of the effects of the electromagnetic interaction on the flow in the channel. The end of Chapter III will contain a discussion of the effects of choking on generator operation.

In Chapter IV, the model developed in Chapter II and the theory presented in Chapter III will be used to develop an understanding of the internal transient response of the generator to changes in load and the effects of choking on terminal characteristics. A possible means of preventing choking while still allowing the desired load changes will then be presented.

Finally, Chapter V will present a summary of the results and conclusions, as well as an outline of possible areas for future research which have been suggested by this work.

CHAPTER II

2.1 Introduction

As discussed in the previous chapter, it is first necessary to develop a model of a constant area MHD generator which reasonably determines the terminal characteristics based on inlet and outlet conditions and physical constraints. Further constraints in the development of the required model are introduced because of the complexity of the defining equations for the system. The derivations will begin with the generalized system of equations, and will then proceed to reduce them to a more numerically tractable form. All quantities, unless otherwise noted, represent quantities measured in the lab frame of the system. (The lab frame is the frame in which the fluid is in motion and the generator is stationary as opposed to the rest frame in which the fluid is at rest).

2.2 Fluid Continuity Equation

Given in (2.1) is the well-known

$$\frac{\partial \rho}{\partial t} = -\nabla\cdot(\rho \underline{V}) \qquad 2.1$$

flow continuity equation, where ρ is the mass density, and $\underline{V}$ is the vector velocity, It should be noted that (2.1) is identical in form and usage to the electric current continuity equation.

2.3 Equation of Motion

The equation of motion is derived by an application of Newton's

Second Law, i.e., the sum of the forces exerted on a body is equal to the rate of change of the momentum of the body. In this case, the body is the fluid of interest and the forces will be body forces, i.e., forces per volume. The complete equation of motion

$$\rho \frac{D\underline{V}}{Dt} = - \nabla P - \rho \nabla \Psi + \nabla \cdot \underset{\leftrightarrow}{\tau}' + \underline{J} x \underline{B} + \rho_e \underline{E} \qquad 2.2$$

is given by (2.2) (Hughes, 1966) where P is pressure, Ψ is gravitational potential, $\underset{\leftrightarrow}{\tau}'$ is the shear part of the mechanical stress tensor, $\underline{J}$ is vector current density, ρ_e is the charge density, $\underline{E}$ is electric field, $\underline{B}$ is magnetic flux density, $\frac{D}{Dt}$ is the substantial derivative and is given by

$$\frac{D}{Dt} = \frac{\partial}{\partial t} + \frac{u\partial}{\partial x} + \frac{v\partial}{\partial y} + \frac{w\partial}{\partial z} \qquad 2.3$$

and

$$\underline{V} = u\underline{i} + v\underline{j} + w\underline{k} \qquad 2.4$$

The left side of (2.2) represents the rate of change of the body's momentum, while the right side represents all forces acting on the body. The first term on the right side represents the pressure gradient acting on the fluid; the second, the gravitational forces; the third, the viscous forces; and the fourth and fifth, the Lorentz force.

2.4 Energy Equation

For the energy equation, a form given by (2.5) (Hughes, 1966) will be used.

$$\rho \frac{De}{Dt} = \Phi - P\nabla\cdot\underline{V} + \nabla\cdot(\kappa_T\nabla T) + \underline{J}'\cdot\underline{E}' \qquad 2.5$$

In (2.5), e represents the specific internal energy, Φ is the mechanical dissipation function which represents the effect of viscosity on internal energy, κ_T is the thermal conductivity, T is temperature, $\underline{J}'$ is current density measured in the rest frame, and $\underline{E}'$ is the rest frame electric field. Kinetic energy effects are not included in (2.5) and will be incorporated into the discussion later.

2.5 Equation of State

The fourth equation is the equation of state modified to account for the presence of two gases rather than one, and is given by

$$P = \frac{1 + \alpha}{\bar{\mu}_o} \rho RT \qquad 2.6$$

where α is the free electron concentration, $\bar{\mu}_o$ is the mean molecular weight, and R is the ideal gas constant (Sutton, 1965).

2.6 Ohm's Law

The fifth and final equation of general interest is Ohm's Law

$$\underline{J} = \sigma(\underline{E} + \underline{V}\mathrm{x}\underline{B}) - \mu(\underline{J}\mathrm{x}\underline{B}) \qquad 2.7$$

where σ is the fluid conductivity and μ is the electron mobility (Sutton, 1965).

2.7 System Configuration and Equations

The MHD duct is configured as Figure 2.1. L is the length of the duct, h is the electrode separation, ℓ is the insulator separation, and B_z represents the applied magnetic field in the z-direction. For this model, both electrode and insulator separation are constant, though not necessarily equal. Variable, finite segmentation of electrodes, connected in the Faraday mode, (Fig. 2.2), is assumed. The flow equations are considered in their one-dimensional form for the solution of the channel flow. Boundary layer effects. which should be treated as three-dimensional flow, are instead approximated by a method to be discussed later.

This one-dimensional approximation of channel flow allows for variation of flow variables in the x-direction only, while assuming that the flow variables, across any cross-section, assume their average value. This averaging will tend to increase the friction and heat transfer effects at the walls, and it is therefore necessary to approximate these effects.

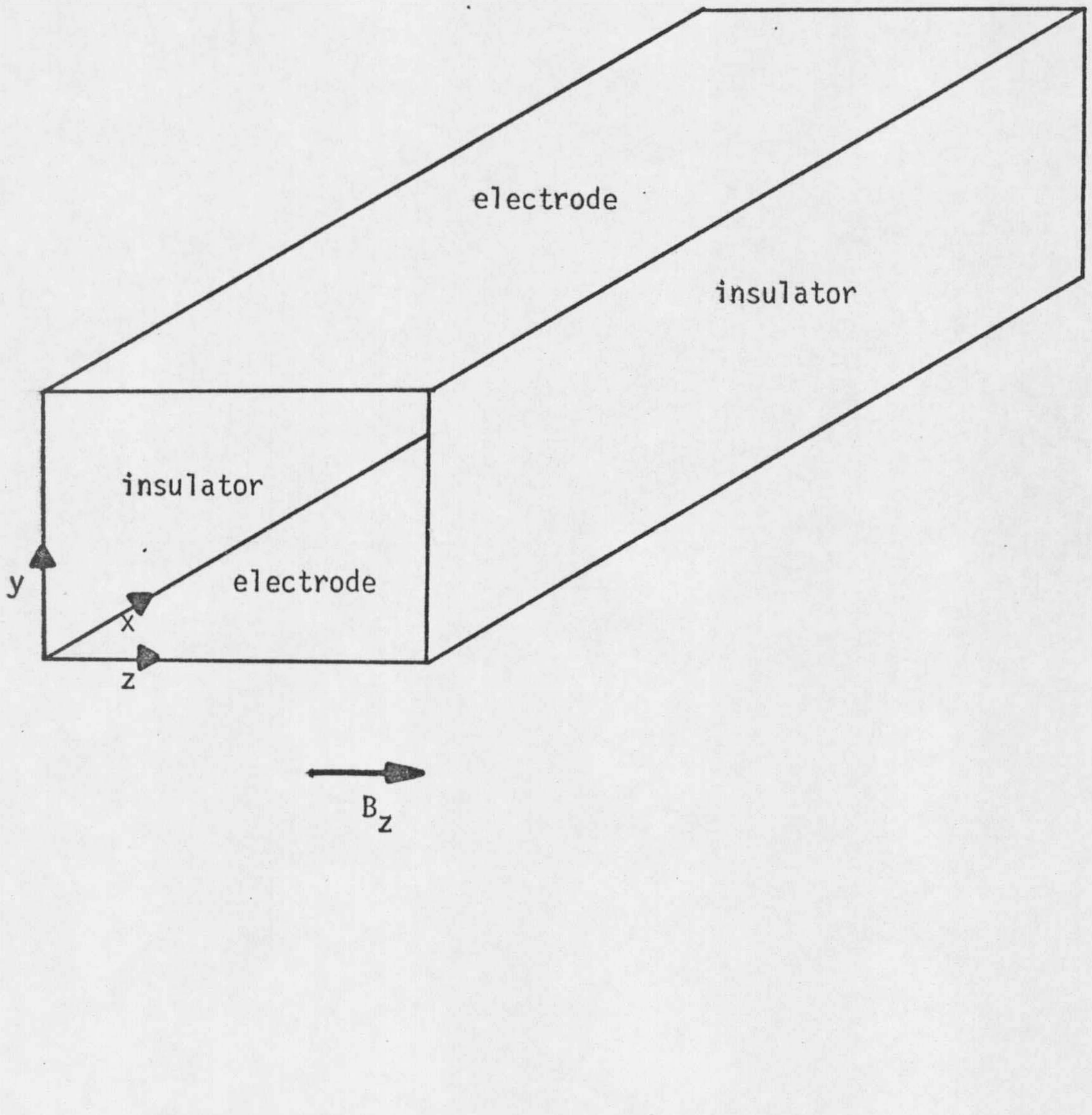

Figure 2.1 MHD Duct Configuration

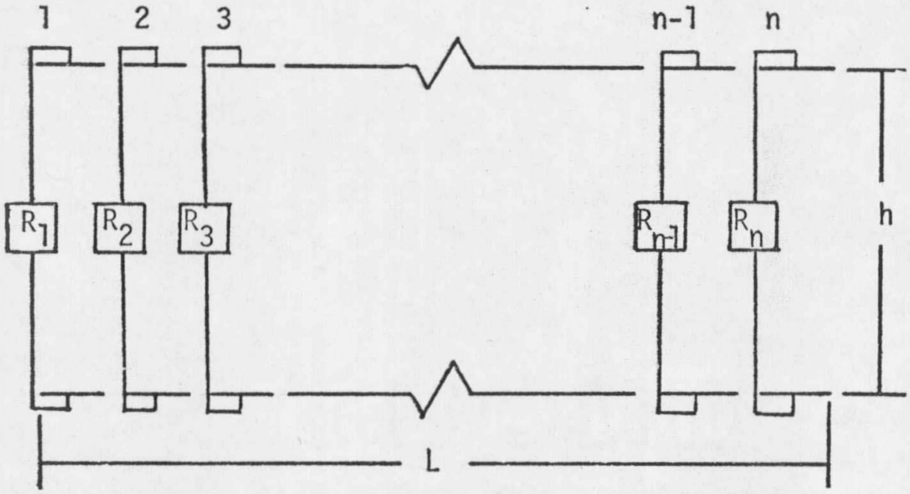

Figure 2.2 Faraday Connected Electrodes

To reduce the defining equations (2.1, 2.2, 2.5) to their one-dimensional form, the y and z derivatives and velocity components are set to zero, to obtain

$$\frac{\partial \rho}{\partial t} = - \frac{\partial \rho u}{\partial x} \qquad 2.8$$

$$\rho \left(\frac{\partial u}{\partial t} + \frac{u \partial u}{\partial x} \right) = - \frac{\partial P}{\partial x} + F + (\underline{J} x \underline{B})_x \qquad 2.9$$

and

$$\rho \left(\frac{\partial e}{\partial t} + \frac{u \partial e}{\partial x} \right) = \Phi - \frac{P \partial u}{\partial x} + Q + \underline{J}' \cdot \underline{E}' \qquad 2.10$$

where F represents the friction effects on the wall, Q represents heat transfer effects, and gravitational and space charge effects have been neglected. The effects of Φ will be discussed later.

The last term on the right side of (2.10) which represents rest frame rather than lab frame quantities is still a problem, but it can be avoided by multiplying (2.9) by u and adding it to (2.10) to get,

$$\rho \left(\frac{\partial e}{\partial t} + \frac{u \partial e}{\partial x} + \frac{u \partial u}{\partial t} + \frac{u^2 \partial u}{\partial x} \right) = - \frac{\partial P u}{\partial x} + Q + \underline{J} \cdot \underline{E} \qquad 2.11$$

where the relation,

$$\underline{J} \cdot \underline{E} = \underline{J}' \cdot \underline{E}' + \underline{V} \, (\underline{J} x \underline{B} + \rho_e \underline{E}) \qquad 2.12$$

has been used with the space charge neglected. In (2.11) the terms Φ and uF have been cancelled since friction can have no effect on the total energy of the system (Pai, 1962). (2.11) can now be rewritten to show more clearly that the energy equation contains both internal and kinetic energy.

$$\rho \left(\frac{\partial(e + u^2/2)}{\partial t}\right) + \rho u \left(\frac{\partial(e + u^2/2)}{\partial x}\right) = - \frac{\partial Pu}{\partial x} + \underline{J}\cdot\underline{E} \qquad 2.13$$

Finally, it is necessary to perform one last manipulation of the flow equations (2.8, 2.9, 2.12) to put them in a form which has useful properties which will be taken advantage of later. It is advantageous to have the variables representing the states on their conservative forms (Roache, 1972). That is, the states should be ρ, m, and E_s, representing mass density, momentum, and stagnation energy, respectively, and defined by

$$m = \rho u \qquad 2.14$$

$$E_s = \rho(e + u^2/2) \qquad 2.15$$

By suitable manipulation of (2.8, 2.9, 2.12) and using the relations (2.14, 2.15), we obtain,

$$\frac{\partial \rho}{\partial t} = - \frac{\partial \rho u}{\partial x} \qquad 2.16$$

$$\frac{\partial m}{\partial t} = - \frac{\partial P}{\partial x} - \frac{\partial m^2/\rho}{\partial x} + F + (\underline{J}x\underline{B})_x \qquad 2.17$$

$$\frac{\partial E_s}{\partial t} = - \frac{\partial\left(\frac{mE_s}{\rho} + \frac{mP}{\rho}\right)}{\partial x} + Q + \underline{J}\cdot\underline{E} \qquad 2.18$$

Expressions for the as-yet undefined terms in (2.17, 2.18) are now presented, and the interested reader should refer to Appendix A for the derivations.

$$(\underline{J}x\underline{B})_x = \sigma u B^2{}_z (K-1) \qquad 2.19$$

$$\underline{J}\cdot\underline{E} = \sigma(uB_z)^2\ K\ (K-1) \qquad 2.20$$

$$K = \frac{E_y}{uB_z} = \frac{1}{1 + \frac{h}{\ell\cdot\Delta x\cdot R_L \sigma}} \qquad 2.21$$

where Δx is the width of one segmented electrode pair, R_L is the corresponding load resistance and K is the loading parameter associated with that electrode pair. Thermodynamic effects are given by

$$F = - \frac{\tau_w C}{A} \qquad 2.22$$

$$\tau_w = (1/2)\frac{m^2}{\rho}\ C_f \qquad 2.23$$

$$C_f = 0.046\ Re^{-0.02} \qquad 2.24$$

$$Re = \frac{mC}{4A\eta} \qquad 2.25$$

$$\eta = 10^{-5}\sqrt{\frac{MT}{1000}} \tag{2.26}$$

$$Q = -\frac{C}{A} N_{st} m C_p (T - T_w) \tag{2.27}$$

and

$$\Phi = \tau_w \frac{\partial m/\rho}{\partial x} \tag{2.28}$$

where τ_w is the average shear stress at the wall, C is the duct perimeter, A is the duct cross sectional area, C_f is the friction factor, Re is the well-known Reynolds number, η is the gas viscosity, M is the Mach number, T is gas temperature, T_w is wall temperature, C_p is specific heat at constant pressure, and N_{st} is the local Stanton number.

The model is now completely described, with two exceptions, by the flow equations (2.16-2.18), the equation of state (2.6), supplemental relations (2.19-2.27), and channel configuration (Fig. 2.1, 2.2). The exceptions are the gas conductivity, σ, which is a function of the thermodynamic states as well as the atomic and physical structure of the working fluid used, and the specific internal energy which is in general a function of pressure and temperature. Because of the complexity of the functional relation for conductivity, calculations of σ are treated by an approximation described in the next section. Calculation of e is also treated in the next section.

2.8 MHD Generator Model

In this section, the development of the one-dimensional model for which the equations were developed in the last section is begun. In the development of this model, two considerations are of overriding importance. First, the model should predict the response of a time-dependent MHD generator reasonably well; and secondly, since the complexity of the defining equations requires a numerical solution of a set of three partial differential equations, all valid approximations and shortcuts should be used. To satisfy the second constraint, several assumptions have been made.

It is assumed that the working fluid of the generator is argon, seeded with cesium. This allows the fluid to be considered as an ideal gas since the specific heat ratio, γ, of a monatomic gas is nearly constant at the temperature being considered (Feynman, 1964). The specific internal energy is then given by

$$e = C_v T \tag{2.29}$$

and γ is given by

$$\gamma = \frac{C_p}{C_v} \tag{2.30}$$

The ideal gas constant, R, is also given by

$$R = C_p - C_v \tag{2.31}$$

Where C_p is the specific heat at constant pressure and C_v is the specific heat at constant volume. Specific internal energy can also be given by

$$e = \frac{RT}{\gamma - 1} \tag{2.32}$$

This choice of a working fluid also allows the conductivity of the gas, σ, to be approximated from a set of graphs (Rosa, 1968). From these graphs it can be seen that σ is dependent on both pressure and temperature. However, since the pressure dependence is slight, the approximation accounts for only temperature variations. The conductivity is approximated by the relation,

$$\sigma = 10^{\left(\frac{x - A}{B - A} + 2\right)} \tag{2.33}$$

where A is the temperature at which $\sigma = 100$ and B is the temperature at which $\sigma = 1000$ (from the graph for which the fluid is A + 0.55% Cs at 3.15 atm). One further simplification will be made in order to better assure the accuracy of the one-dimensional assumption and also to avoid any problems with separation in the flow. The channel is assumed to be of constant cross-sectional area. With these final simplifications in hand, the actual integration of the defining equations is now considered.

For the integration of the time-dependent equations, a two-step Lax-Wendroff method (Roache, 1972) will be slightly modified to include the electromagnetic effects. This Lax-Wendroff method has given excellent results in the solution of ordinary fluid dynamics problems, and there is no reason to expect that the results will be any less excellent when the method is applied to MHD flow.

Before applying the scheme, however, it is convenient to put the defining equations (2.16-2.18) in a shorthand notation given by

$$\frac{\partial \underline{U}}{\partial t} = \frac{-\partial \underline{F}(\underline{U})}{\partial x} + \underline{G}(\underline{U}) \qquad 2.34$$

and,

$$\underline{U} = \begin{bmatrix} \rho \\ m \\ E_s \end{bmatrix} \qquad 2.34a$$

$$\underline{F}(\underline{U}) = \begin{bmatrix} m \\ \frac{m^2}{2\rho}(3 - \gamma) + (\gamma - 1)E_s \\ \frac{m}{\rho}(\gamma E_s - (\gamma - 1)\frac{m^2}{2\rho} \end{bmatrix} \qquad 2.34b$$

$$\underline{G}(\underline{U}) = \begin{vmatrix} 0 \\ F + (\underline{J}x\underline{B})_x \\ Q + \underline{J}\cdot\underline{E} \end{vmatrix} \qquad 2.34\text{ c}$$

where m and E_s are defined by (2.14-2.15) and P has been replaced by

$$P = (\gamma - 1)\, E_s - \frac{m^2}{2\rho} \qquad 2.35$$

using (2.6), where α, the percent of ionization, is assumed to be neglible.

Given the initial and boundary conditions, the first step of the Lax-Wendroff method is used to advance the solution one-half time step (see Figure 2.3) using

$$\underline{u}_{i+1/2}^{n+1/2} = \left[\frac{\underline{u}_{i+1}^{n} + \underline{u}_{i}^{n}}{2}\right] - \frac{\Delta t}{2}\left[\frac{\underline{F}_{i+1}^{n} - \underline{F}_{i}^{n}}{\Delta x} - \frac{\underline{G}_{i+1}^{n} + \underline{G}_{i}^{n}}{2}\right] \qquad 2.36$$

This gives values for the states at intermediate points in the mesh. Using these values and the initial values at the mesh points, the solution is advanced one complete time step using

$$\underline{u}_{i}^{n+1} = \underline{u}_{i}^{n} - \Delta t\left[\frac{\underline{F}_{i+1/2}^{n+1/2} - \underline{F}_{i-1/2}^{n+1/2}}{\Delta x} - \frac{\underline{G}_{i+1/2}^{n+1/2} + \underline{G}_{i-1/2}^{n+1/2}}{2}\right] \qquad 2.37$$

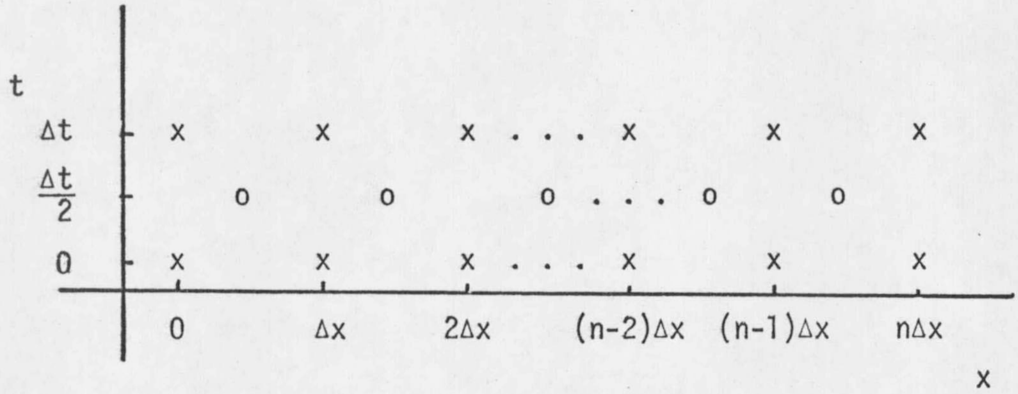

Figure 2.3 Outline of the Two-step Lax-Wendroff Method

The solution is now advanced in time as far as required by iterating with this scheme. This method of solution has powerful features which should be noted, so that they can later be used to an advantage. First, this finite-difference scheme is conservative, and this, when coupled with the use of conservation variables, guarantees that proper jump conditions across a shock in the fluid will be obtained (Roache, 1972). Because of this, the method is also applicable to transonic flow. Secondly, the method has an artificial damping effect which tends to stablize calculations across shocks.

The usual stability constraint must still hold to allow a stable solution, where u is fluid velocity and c is the sonic speed.

$$|u| + c < \frac{\Delta x}{\Delta t} \qquad 2.38$$

2.4 Initial and Boundary Conditions

The two-step method for the solution of the time-dependent equations is nearly useless, however, if a set of reasonably accurate initial conditions is not available. It is noted by Roache (1972) that instabilities can occur for some initial conditions and not for others. He suggests this may be caused by spurious shock propagation due to poor initial conditions. Unfortunately, however, very little work seems to have been done on methods of calculating initial conditions.

For this reason, and because Runge-Kutta methods are popular and well-known, a fourth order Runge-Kutta scheme (Gerald, 1970) is used to calculate the initial conditions using the steady state form of (2.34). This solution is propagated in time for five time steps at which point a steady state condition is assumed to be reached as the change in total power output for one time step is less than four percent. Unfortunately, this Runge-Kutta method is unable to give correct results for transonic conditions in a constant area generator.

The determination of the outlet boundary conditions is straightforward, as it is assumed that the stagnation pressure is fixed if the flow is subsonic and the outlet is completely free to change if the flow is supersonic. This is accomplished using a backward difference scheme of the form for the outlet calculation. The constraint on the

$$\underline{u}_i^{n+1} = \underline{u}_i^n - \Delta t \left[\frac{\underline{F}_i^n - \underline{F}_{i-1}^n}{\Delta x} - \underline{G}_i^n \right] \qquad 2.39$$

stagnation pressure is easily met by holding E_s, at the outlet, constant for subsonic flow.

The determination of the inlet boundary condition is more complex because after several tests, it was found that neither a fixed nor a free boundary condition on $\underline{U}$ at the inlet, gave consistent results in all cases. It was therefore necessary to add a nozzle to the generator between the reservoir, (representing the heat exchanger), and the inlet to the MHD generator. Since this nozzle is of a converging nature, it is necessary to further modify the defining one-dimension equations by the addition of terms to account for the area variation. This is done in much detail by Pai (1962) and therefore will not be reproduced here. Equation (2.34) then becomes

$$\frac{\partial \underline{U}}{\partial t} = - \frac{\partial}{\partial x} \underline{F}\ (\underline{U}) - \underline{H}\ (\underline{U}) \frac{1}{A} \frac{\partial A}{\partial x} + \underline{G}(\underline{U}) \qquad 2.40$$

where

$$\underline{H}\ (\underline{U}) = \begin{bmatrix} m \\ \frac{m^2}{\rho} \\ \frac{m}{\rho} (\gamma E_s - (\gamma - 1) \frac{m^2}{2\rho} \end{bmatrix} \qquad 2.40a$$

This new system can be solved easily using the established methods by defining a $\underline{G}^*$, given by

$$\underline{G}^*\ (\underline{U}) = \underline{G}\ (\underline{U}) + \underline{H}\ (\underline{U}) \frac{1}{A} \frac{\partial A}{\partial x} \qquad 2.40b$$

where A is the cross-sectional area. All other terms have their usual meanings. With the addition of the nozzle, it is still necessary, however, to establish boundary conditions, at the inlet to the nozzle.

Since the fluid at this point is nearly stationary and the nozzle inlet is somewhat isolated from the generator inlet, the three states. ρ, m, and E_s, at the nozzle inlet will all be held fixed.

The composite system is now given in Figure 2.4 and has several properties which should be noted. First, since the nozzle is entirely convergent and the MHD channel is constant in cross section, the flow will be entirely subsonic. Secondly, the inlet and outlet reservoirs are assumed to be large enough to absorb any changes, due to fluid flow, without effect. That is to say, P_o, T_o, and P_e are all constant and represent stagnation values.

A model is now available which is able to predict with some degree of accuracy, the time-dependent response of an MHD generator subject to various changes in operating conditions. In the next chapters, this model will be used to enable us to develop an understanding of the phenomena of choking and its effects on an MHD generator.

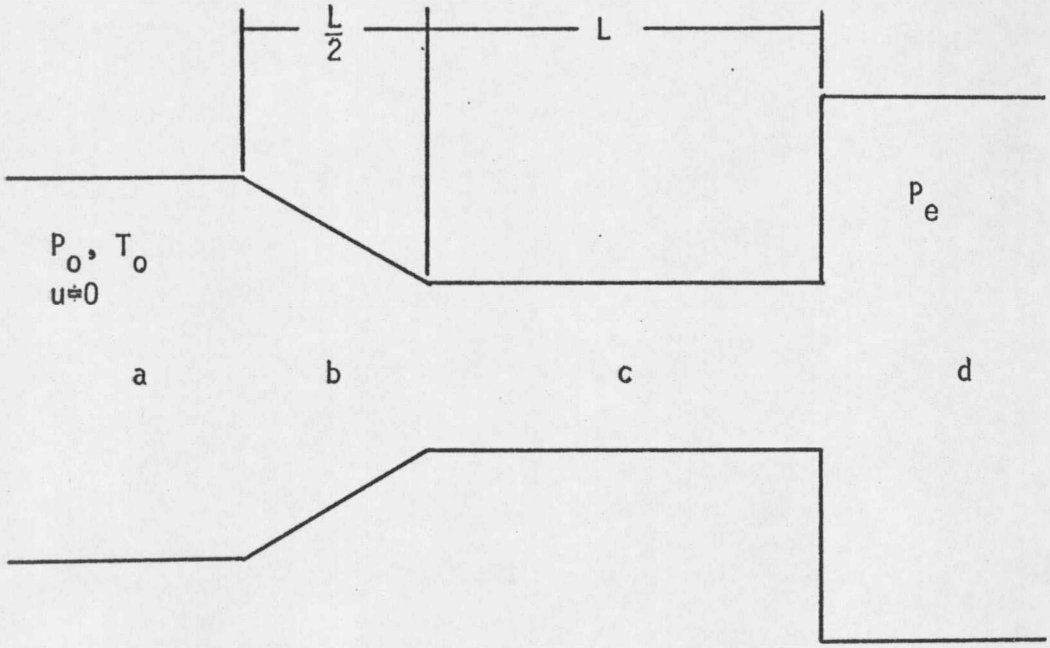

Figure 2.4 Final System Schematic with (a) Inlet Reservoir, (b) Subsonic Nozzle, (c) MHD Generator, and (d) Outlet Reservoir

CHAPTER III

3.1 Introduction

In this chapter, choking and why it occurs will be studied in some detail. The effects and possible consequences of choking in an MHD generator will then be looked into, based on the understanding of choking developed in the first section.

Choking, sometimes called the critical state, can be defined in several ways, all of which are comparable. It can be defined as having occurred if the mass flow rate has reached its maximum at some point in the channel, or if the Mach number is one in the absence of a throat. Choking can also be said to have occurred in the channel, if the pressure ratio (P_e/P_o) is less than the critical value for the flow.

Chapman and Walker (1971) develop an explanation of choking, for both subsonic and supersonic flow, based on the pressure ratio, and since this appears to be the most easily understood, it is the method which will be adopted here. The supersonic case, however, will be ignored as the generator design which will be used is for subsonic flow only. The interested reader should refer to Chapman and Walker for the material on supersonic flow.

3.2 Choking-The Critical State

Consider a channel of the form given by Figure 3.1 (a). For the moment, assume that the flow is adiabatic. Figure 3.1 (b) then gives the pressure variation for various exit pressures. Curve 'a' gives the

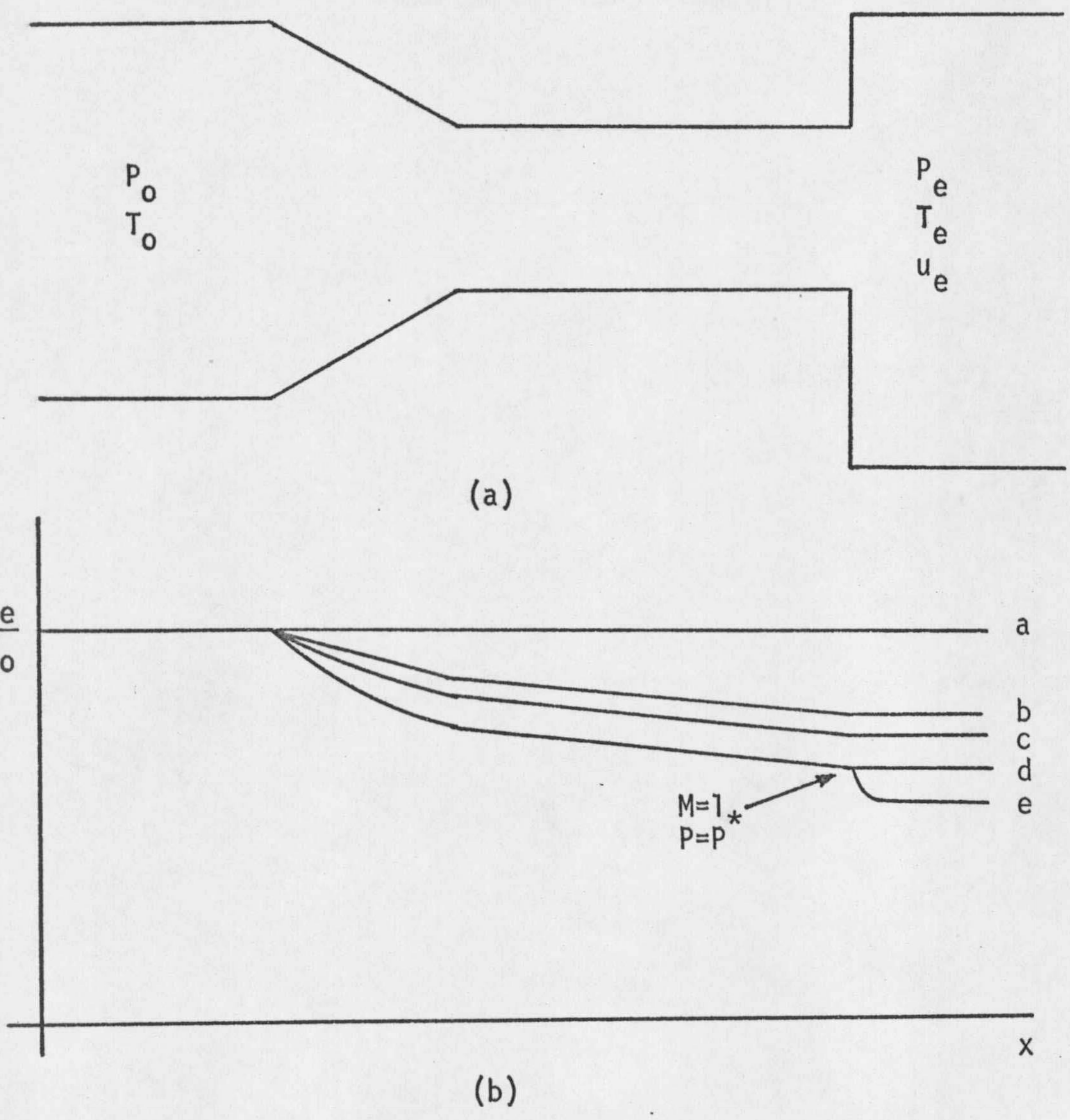

Figure 3.1 Effects of Pressure Ratio on Fluid Flow
(a) Channel Configuration (b) Pressure Distribution

ratio when the exit pressure is equal to the stagnation pressure. Curves 'b', 'c', and 'd' give the pressure ratio as the exit pressure is decreased until it equals the critical pressure, P*. At this point, the flow is choked and any further decrease in the exit pressure will not affect the flow upstream of the choke, as can be seen from curve 'e'. Physically, this can be easily seen to be due to the fact that, when it chokes, the fluid is flowing at the speed of sound and the speed of sound is the rest frame velocity at which pressure disturbances propagate. These two occurrences cause the relative velocity of propagation of a pressure wave upstream to be zero. That is, the fluid downstream from the choke is effectively isolated from the fluid upstream. The pressure ratio at which this occurs is called the first critical pressure ratio. Two further pressure ratios are also usually defined but will be ignored here since they only have meaning for supersonic flow.

Before the concept of a pressure ratio can be used to any advantage, however, it is necessary that an understanding of the effects of friction and heat losses on the pressure ratio be understood. It is first necessary though, to establish some basics and outline the restrictions on the discussion to be presented.

For convenience, define an operating or applied pressure ratio, denoted by r_o, and denote the critical pressure ratio by r_{cp}. For subsonic flow to exist without choking

$$1 > r_o > r_{cp} \qquad 3.1$$

must be satisfied. For $r_{cp} \geq r_o$, the flow will choke.

Before continuing, it should also be noted that any comments concerning choking which are made concerning friction effects will apply directly to $\underline{J} x \underline{B}$ forces, and electrical energy extraction can be treated exactly as heat losses. This can be seen immediately from (2.17-2.18). It should also be stressed that, in general, all remarks apply only to subsonic flow and do not necessarily hold for supersonic flow. Care should also be taken to distinguish between steady state phenomenon and transient phenomenon, as will be pointed out later. With these cautions in mind, an understanding of the factors which influence choking in the steady state case will now be developed.

3.3 Steady State Effects

The effects of friction and heat losses on steady flow are outlined in Tables 3.2 and 3.3 and since these factors are discussed in much detail elsewhere (Shapiro, 1953), their effects will only be summarized below. Friction tends to increase the critical pressure ratio and thereby increase the likelihood of choking, while heat losses have just the opposite effect. Of course, the combined effect depends on the relation magnitudes of each effect and therefore cannot be treated in a general discussion.

The effects of the $\underline{J} x \underline{B}$ and $\underline{J} \cdot \underline{E}$ terms on steady flow are not so directly analyzed, however, as they, in general, do not exist independently.

Table 3.2. Effect on the Steady-State Flow Parameters in a Constant Area Channel Due to Friction Only (M<1).

Pressure (P)	decreases
Temperature (T)	decreases
Velocity (u)	increases
Mach Number (M)	increases

Table 3.3. Effect on the Steady-State Flow Parameters in a Constant-Area Channel Due to Heat-Loss Only.(M<1).

Pressure (P)	increases
Temperature (T)	note *
Velocity (u)	decreases
Mach Number (M)	decreases

---

*decreases for $M<1 / \sqrt{\gamma}$, and increases for $M>1 / \sqrt{\gamma}$

Because of this coupling, the influence of these factors on the critical pressure ratio, for various values of loading, is determined by the numerical integration of the steady state flow equations using the Runge-Kutta method described in Chapter II. (See Appendix D for program). Friction and heat losses are neglected in the analysis since the influence of electromagnetic effects is being studied. The results are summarized in Figure 3.4. Several things should be emphasized based on these results. It is noted from 3.4 (b) that choking due to electromagnetic effects is strongly dependent on duct length as well as the pressure ratio. It is also obvious from 3.4 (b) and 3.4 (c) that a reduction in K will tend to move the point at which choking will occur toward the inlet and at the same time will tend to increase the critical pressure ratio, both effects which will tend to make choking more likely to occur. An increase in K will tend to have just the opposite effect. With these general steady state effects in mind, we will now begin to develop a basic understanding of the transient response of an MHD generator, based on the defining equations.

3.4 Transient Effects

A preliminary understanding of the transient effect can be obtained by considering equations (2.2,2.5) reduced to their one-dimensional form.

$$\rho \frac{\partial u}{\partial t} = - \rho u \frac{\partial u}{\partial x} - \frac{\partial P}{\partial x} + F + (\underline{J} x \underline{B})_x \qquad 3.2$$

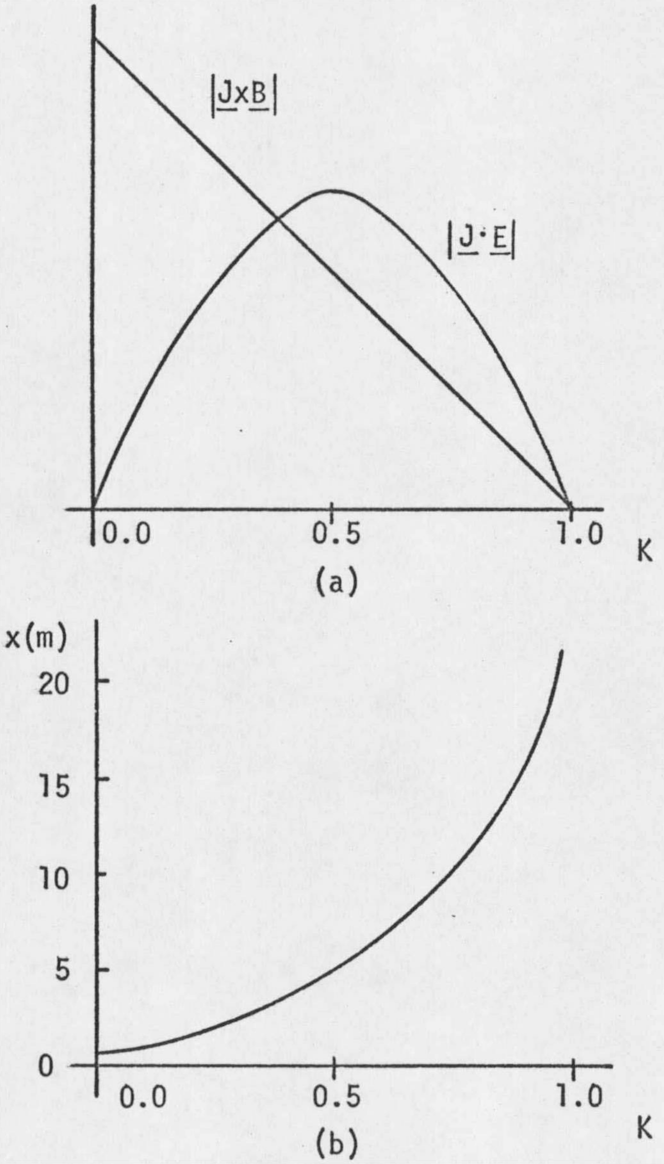

Figure 3.4 (a) Variation of $|\underline{J}\times\underline{B}|$ and $|\underline{J}\cdot\underline{E}|$ with K
(b) Variation of length of duct needed to choke flow with K
(c) Variation of r_{pc} with K
P_o=4.5 atm, T_o=2850^{o}K

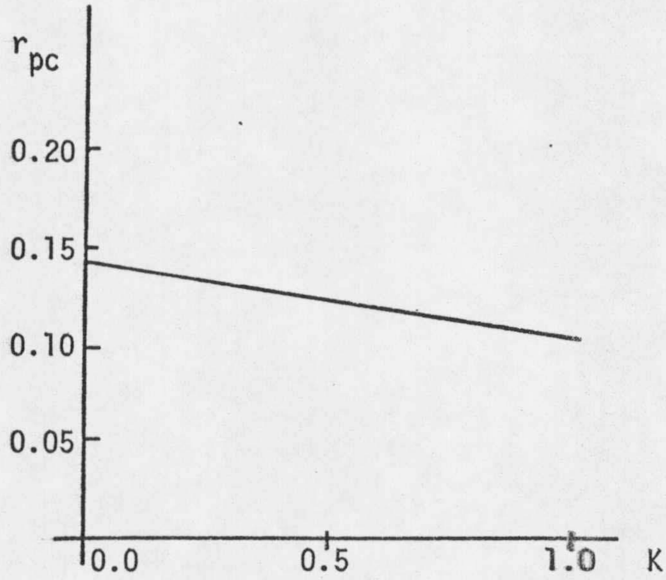

(c)

Figure 3.4 (cont.)

$$\rho C_v \frac{\partial T}{\partial t} = - \rho u C_v \frac{\partial T}{\partial x} - P \frac{\partial u}{\partial x} + Q + \underline{J}'\cdot\underline{E}' \tag{3.3}$$

Now $\underline{J}'\cdot\underline{E}'$ can be represented by

$$\underline{J}'\cdot\underline{E}' = \underline{J}\cdot\underline{E} - u(\underline{J}\mathrm{x}\underline{B})_x \tag{3.4}$$

or, for a Faraday-connected generator

$$\underline{J}'\cdot\underline{E}' = \sigma u^2 B^2 (K-1)^2 \tag{3.5}$$

where

$$(\underline{J}\mathrm{x}\underline{B})_x = \sigma u B^2 (K-1) \tag{3.6}$$

$$\underline{J}\cdot\underline{E} = \sigma u^2 B^2 K(K-1) \tag{3.7}$$

If it is assumed, for a Faraday-connected generator, that the flow is fully developed, steady state and that the loading factor, K, is constant throughout the channel, the following is easily seen.

Increasing K uniformily will, initially at least, increase $(\underline{J}\mathrm{x}\underline{B})_x$ which will tend to increase the velocity, u. Increasing K will also tend to decrease $\underline{J}'\cdot\underline{E}'$, thereby decreasing temperature, T. Decreasing K will tend to have just the opposite effect.

This means that an increase in K will tend to increase the probability of choking and a decrease in K will have just the opposite effect. This, however, is exactly opposite of what would be expected based on the steady state analysis. This apparent conflict, however, is easily resolved if it is realized that the only boundary condition which is allowed to vary was the electrical load, and the flow is still constrained to satisfy the original pressure ratio. What happens as both of these boundary conditions are varied will be a point of discussion in Chapter IV.

For the time being, this will be the extent of the discussion on the transient response of an MHD generator. With the preliminary understanding of choking just developed, some of the consequences of choking in an MHD generator will be now considered.

3.5 Choking in an MHD Generator

Consider an MHD generator of the configuration given in Figure 3.5. This configuration is of the general type which would be used for a subsonic generator. Section (a) is a nozzle to reduce the pressure and increase the velocity of the working fluid as it comes out of the heat exchanger or combustor, which would preceed the MHD generator. Section (b) is the MHD channel itself where energy is extracted. For subsonic flow, this is usually of a slightly divergent nature, such that the flow velocity is maintained near, yet below, Mach one. Section (c) is the subsonic diffuser to decrease the flow velocity and increase the

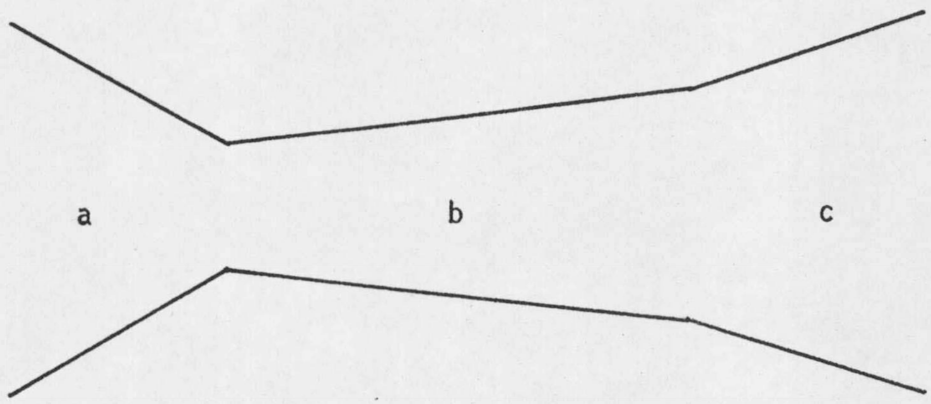

Figure 3.5 MHD subsonic channel configuration
(a) Nozzle (b) Generator (c) Diffuser

fluid pressure, such that the fluid state would be suitable for a heat exchanger which would usually follow the MHD generator.

Based on the properties of subsonic nozzles and diffusers, it can be easily shown that the point of maximum Mach number (for the subsonic case), must occur at the inlet or outlet of the MHD generator or interior to the MHD generator itself (Section (c), Figure 3.5). It further follows that if the flow chokes because of electrical load changes, it will first choke in the MHD generator itself and the choke will eventually tend to be carried toward the end of the channel. However, as the choke moves into the diffuser section, several things will begin to happen.

The flow will first develop into three basic regions:

a - subsonic upstream region

b - supersonic intermediate region

c - subsonic downstream region.

As these three regions move into the diffuser, regions 'a' and 'c' will be de-accelerated while region 'b' will be accelerated. This will immediately cause a compression shock to begin to develop between regions 'b' and 'c'. At this point, several things could happen, dependent on the applied pressure ratio. The flow could become entirely supersonic downstream of the choke and into the heat exchanger. In this case, the shock will preceed the supersonic region and therefore move into the heat exchanger also. The flow could also remain separated into three regions in the channel with the shock remaining fixed in position or moving to another stationary position.

No matter what happens, however, problems will arise. In the first case, a heat exchanger which was designed for low velocity flow will be subject to supersonic flow and will in all likelihood be damaged, if not entirely ruined. In the second case, the shock is causing additional stresses on the MHD channel which has already had to be built to cope with the severe stresses of normal operation.

In any case, the problem of how to restore the channel to normal operation is now present and the problem is complicated, in the second case, by the existence of a shock in the channel.

Based on the above discussion, it should be apparent that choking should be avoided if at all possible. With this in mind, Chapter IV will begin a study of choking using the model developed in Chapter II.

CHAPTER IV

4.1 Introduction

In this chapter, two major areas will be covered. First, the transient response of an MHD generator to various load changes will be studied using the model developed in Chapter II. Second, a possible means of compensating for these load changes will be developed and analysed using the same model.

4.2 Model Configuration

Before proceeding with the analysis, it is first necessary, however, to define the configuration of the MHD channel. This is done in Table 4.1, which gives the basic configuration of the channel, and in Appendix C, which lists and explains the FORTRAN-IV program used to implement the model. No mention is made in Table 4.1 of the outlet boundary conditions as they are initially dependent on the electrical loading of the generator.

4.3 Generator Transient Response

To study the transient response of an MHD generator, it is first necessary to establish an operating condition and to then study the behavior of the generator as parameters are changed such that the generator moves off the steady state operating condition.

To establish the steady state operating condition, the generator was uniformily loaded such that the loading factor, K was one-half.

This corresponds to the theoretical point of maximum power transfer (see Appendix B). A summary of the outlet conditions, for this loading, is given in Table 4.2. This loading gave a total power output of 21.36 MW. Figures 4.3 (a,b,c,d, and e) give the distribution of voltage, current, momentum density, pressure and temperature for the length of the MHD channel.

From this steady state operating condition, two types of transient response were considered, the open-circuit case (K = 1), and the short-circuit case (K = 0). Figures 4.4. and 4.5, respectively, give the variation of several parameters for these two cases. Of the two cases, the open-circuit case is of the most interest here as it tends to increase the likelihood of choking in the generator.

Several things are immediately obvious from these graphs. From 4.4(a) and 4.5(a), it is apparent that the momentum density is constant in the MHD generator (2 - 6 meters) when the generator is in steady state. This is therefore an indicator as to the state of the generator after a disturbance has occurred.

From Figures 4.4(c) and 4.4(d), the process which occurs during choking is made somewhat clearer. As the flow chokes, the critical point initially moves upstream, causing a supersonic region to develop. Eventually, the critical point will stop its upstream motion and will move downstream to the end of the MHD generator. As this occurs, the supersonic region, downstream of the critical point, will move into the

Table 4.1. MHD Duct and Nozzle Configuration

(1) Geometry	
Nozzle	
Length	2 m
Cross-Section area, inlet	2.56m^2
Cross-Section area, outlet	.64m^2
Area Variation	quadratic
Generator	
Length	4 m
Cross-Section Area, inlet	.64m^2
Cross-Section Area, outlet	.64m^2
Area Variation	constant
Electrode Width	.13m
Electrode Length	.8 m
No. of Electrodes	30
(2) Inlet and Wall Boundary Conditions	
Inlet Pressure	4.5 atm
Inlet Velocity	29.4 m/s
Inlet Temperature	2800^{o}K
Inlet Mach Number	.03
Wall Temperature	1000^{o}K

Table 4.1. (Continued)

(3) Gas and Electrical Parameters

Percent Argon	99.45%
Percent Cesium	.55%
Inlet Conductivity	158.5 mhos/m
Specific Heat Ratio (γ)	1.67
Ideal Gas Constant	$8.205 \times 10^{-5} \frac{m^3 \cdot atm}{mole \cdot {}^\circ K}$
Stanton Number	0.00032
Magnetic Field	3.0T
Electrode Voltage Drop	0.0V
Electrode Configuration	Faraday (segmented)

Table 4.2. Outlet Conditions for K = 1/2

Pressure	.88 atm
Pressure, Stagnation	1.01 atm
Velocity	425.7 m/s
Temperature	1937 °K
Mach Number	.52

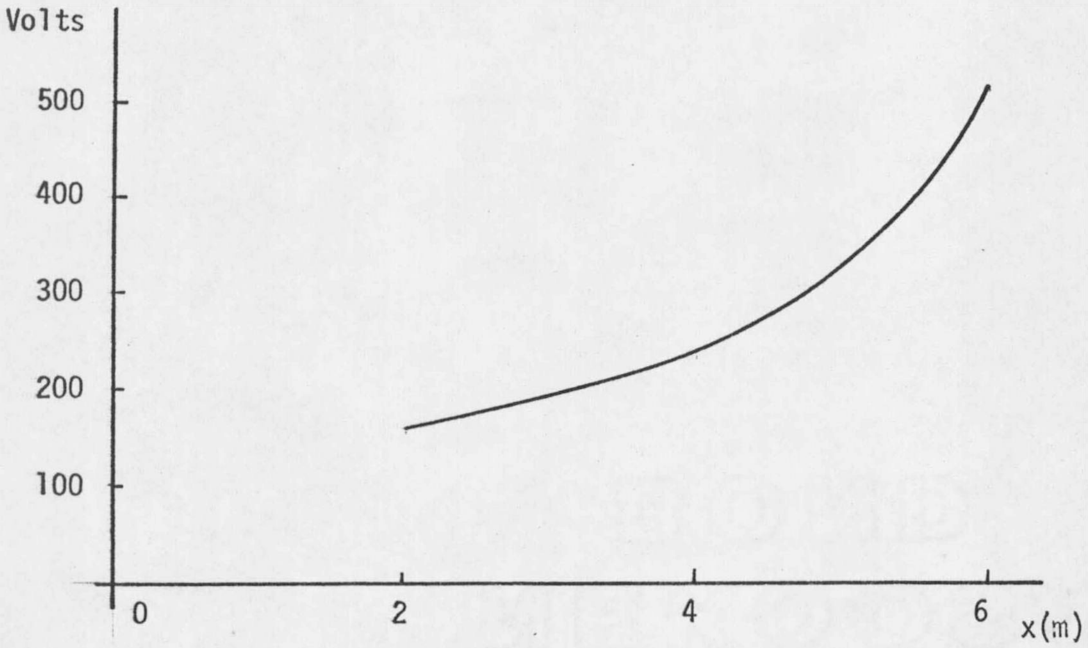

(a) Voltage Variation

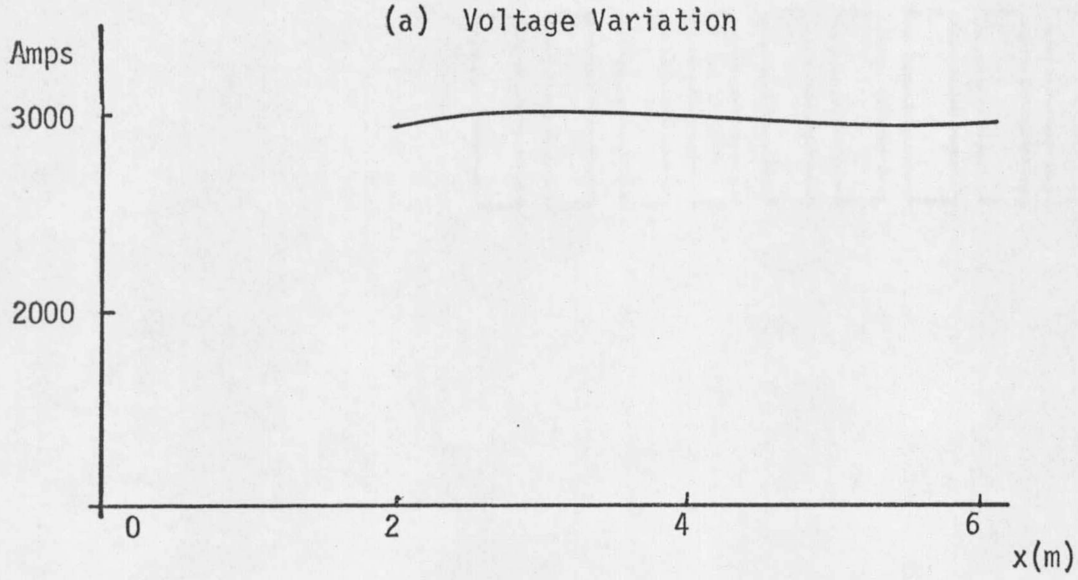

(b) Current Variation

Figure 4.3 Several Steady State Parameters as a Function of Distance

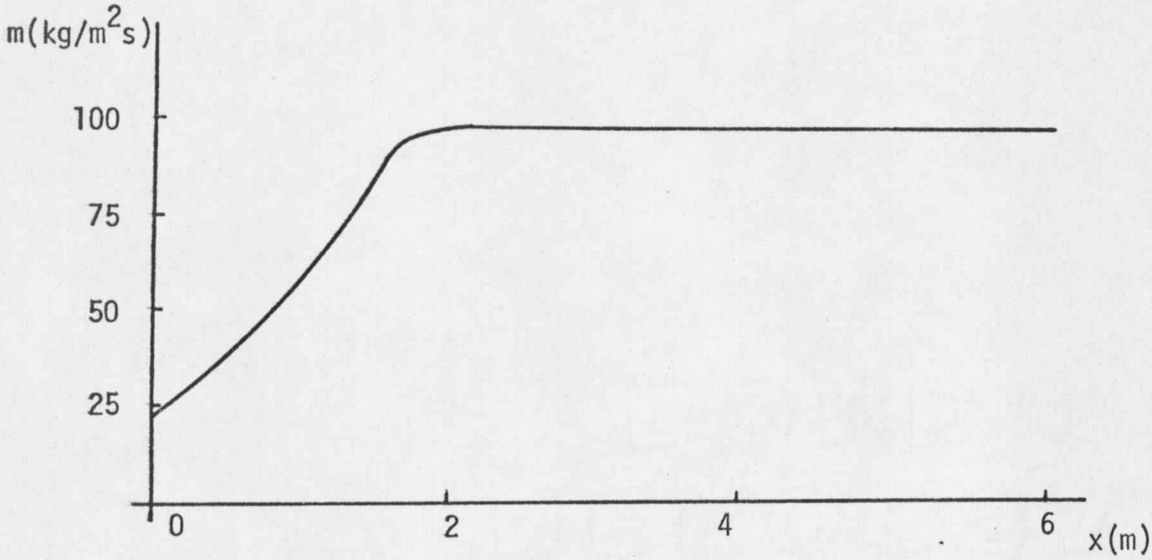

(c) Momentum Density Variation

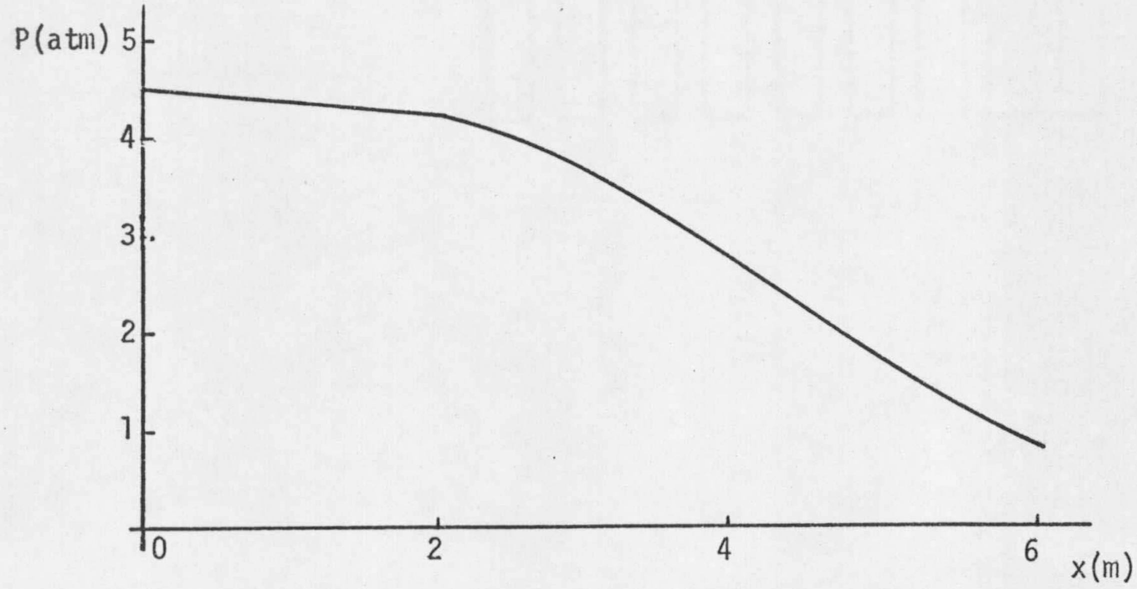

(d) Pressure Variation

Figure 4.3 (cont.)

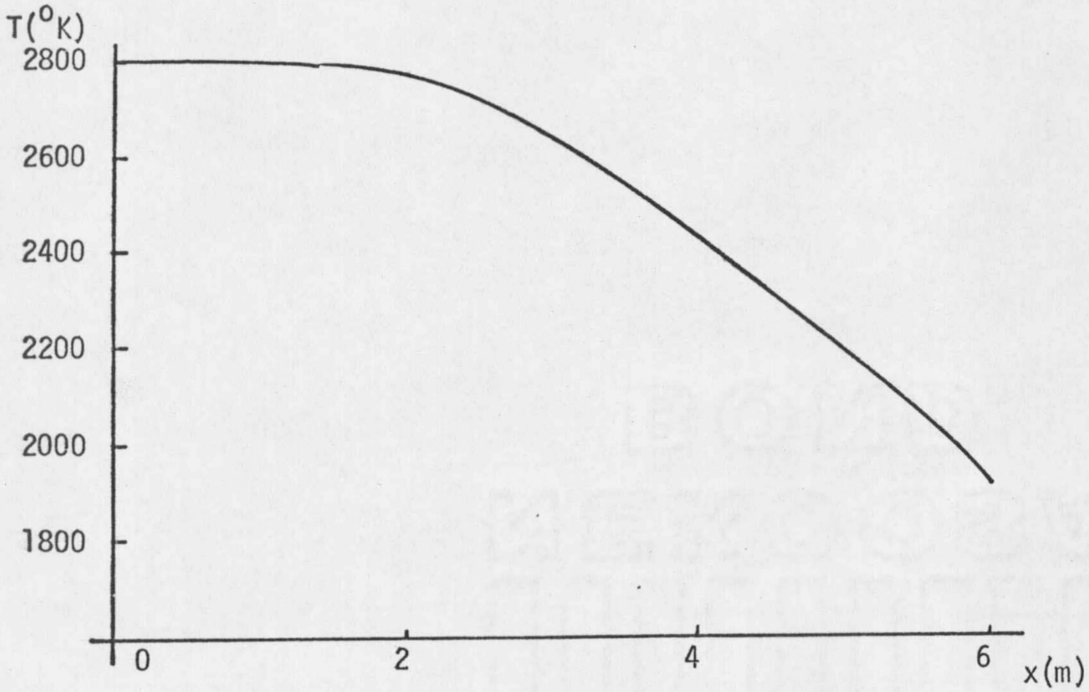

(e) Temperature Variation

Figure 4.3 (cont.)

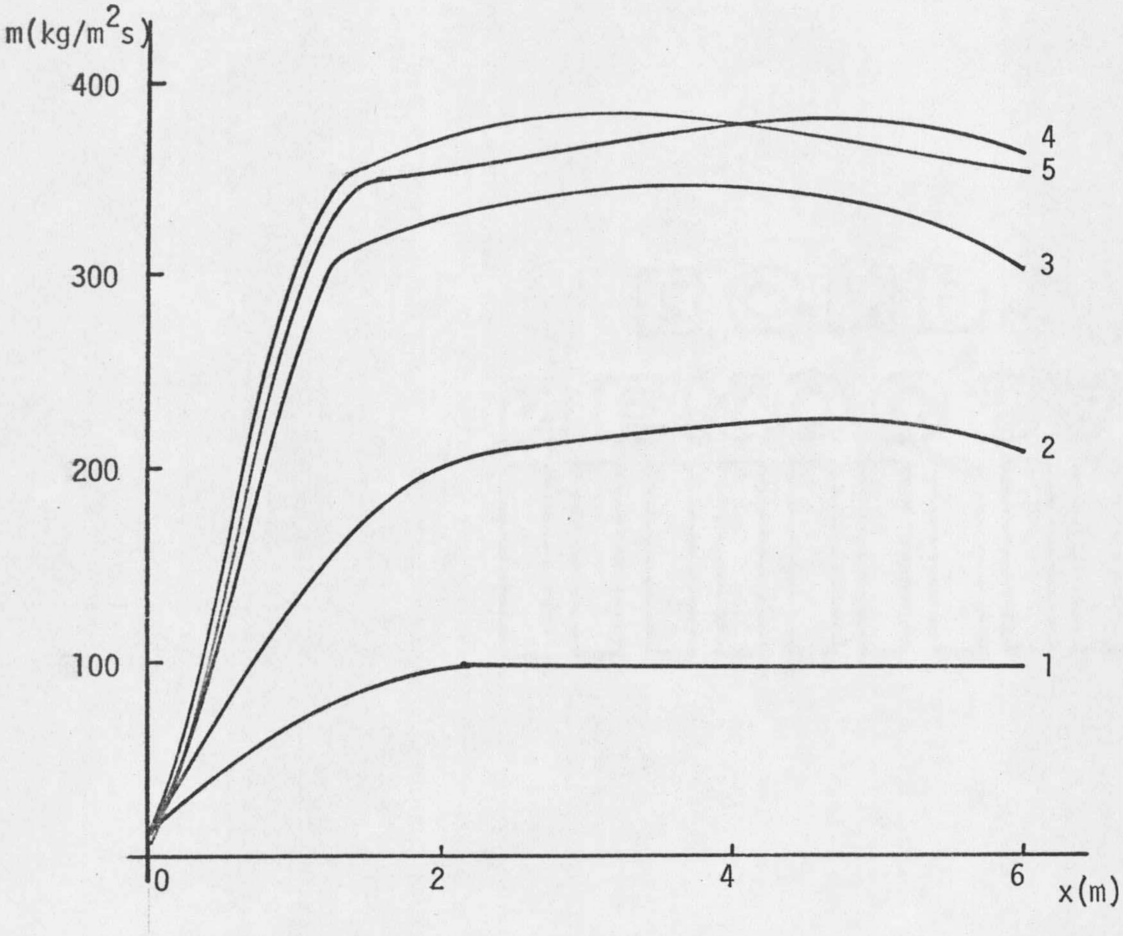

(a) Variation of Momentum
Density with Distance

Figure 4.4 Response of MHD generator to change in load from K=0.5 to K=0.999. (1) t=0.2 msec (2) t=4 msec (3) t=8 msec (4) t=16 msec (5) t=24 msec

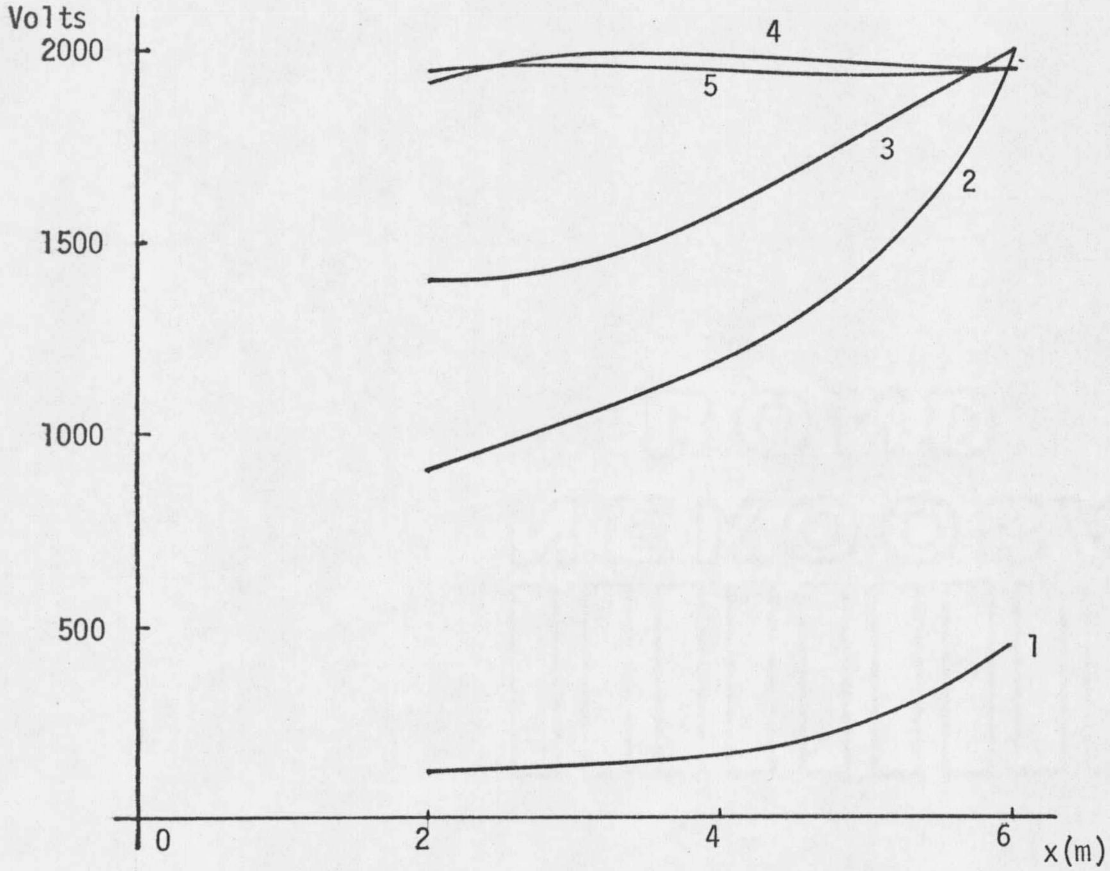

(b) Variation of Voltage with Distance

Figure 4.4 (cont.)

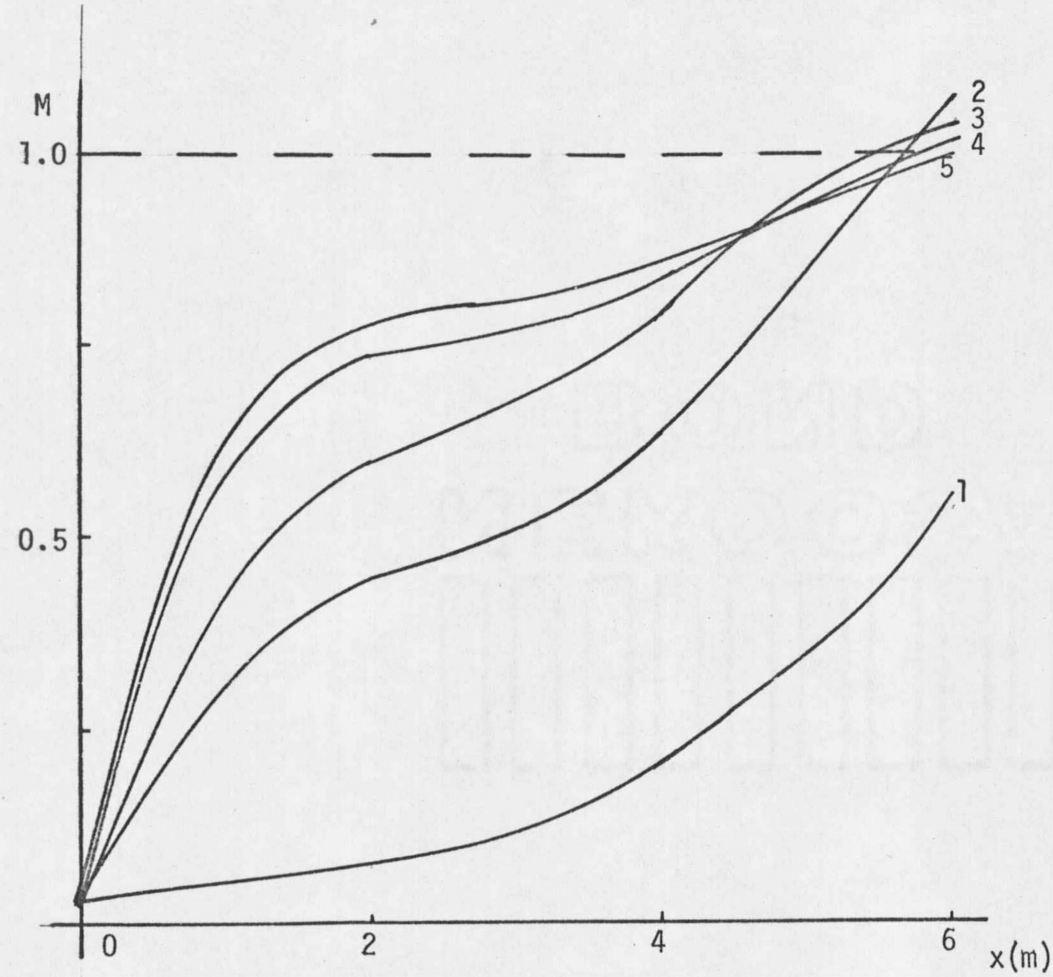

(c) Variation of Mach Number with Distance

Figure 4.4 (cont.)

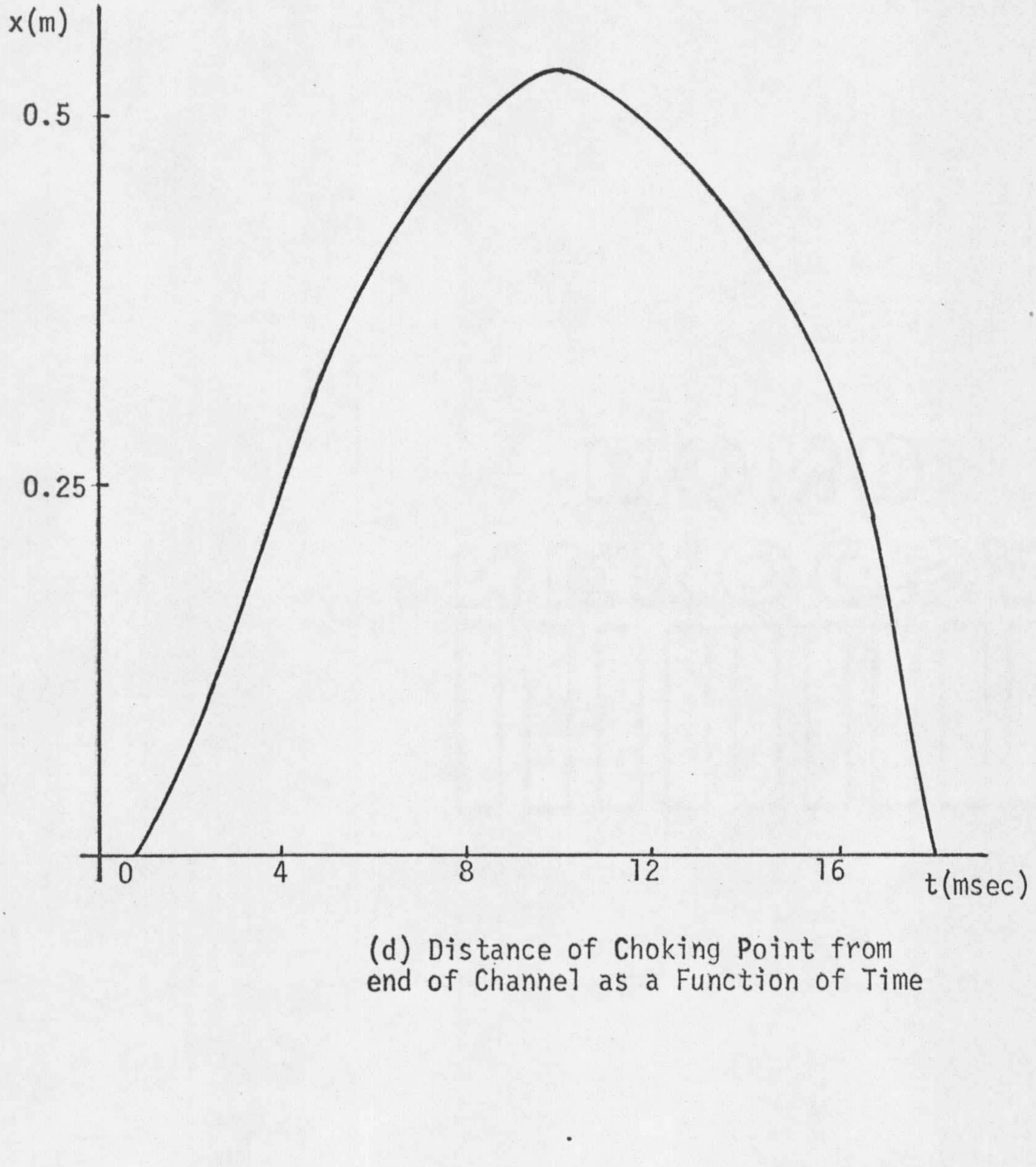

(d) Distance of Choking Point from end of Channel as a Function of Time

Figure 4.4 (cont.)

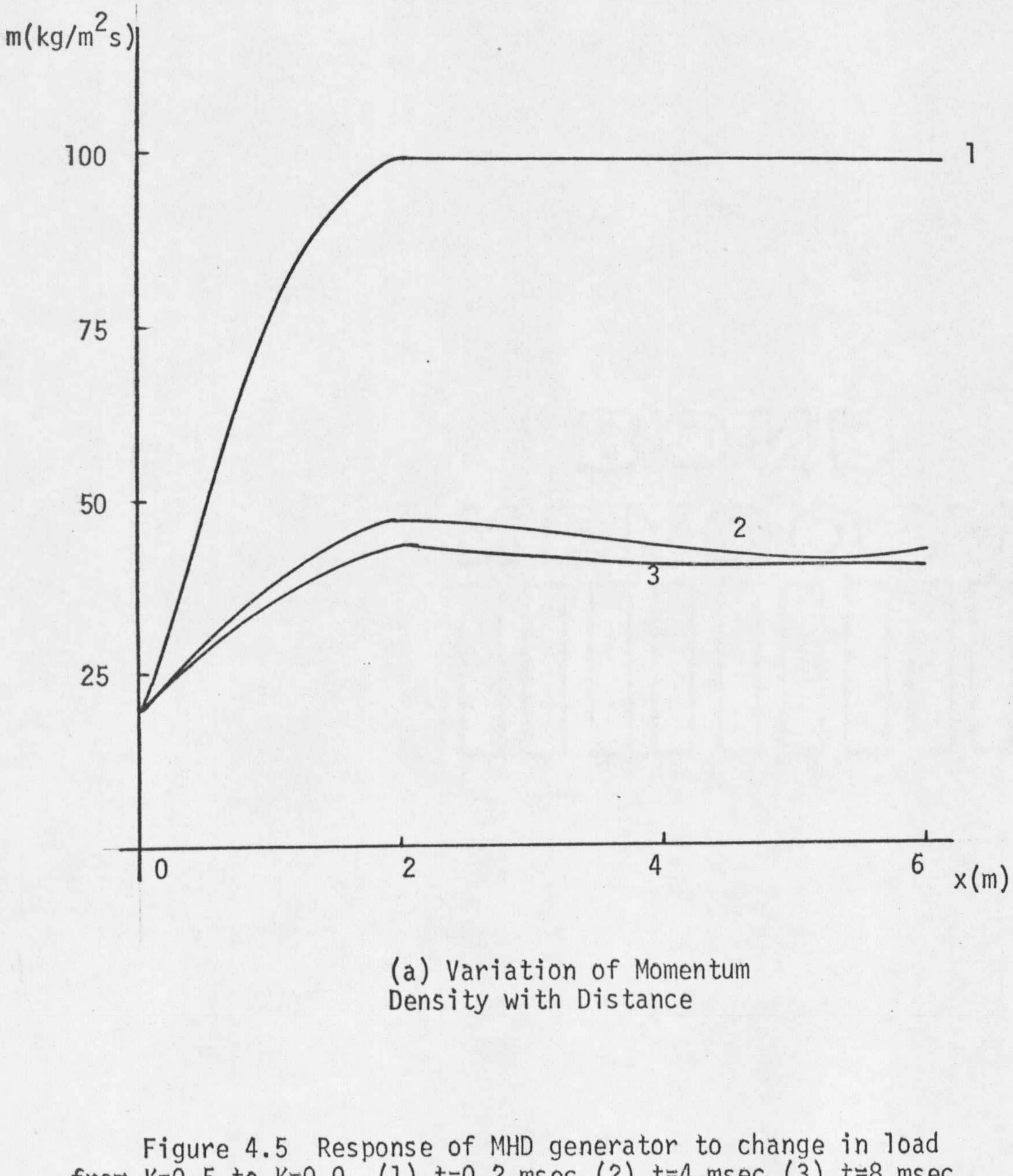

(a) Variation of Momentum
Density with Distance

Figure 4.5 Response of MHD generator to change in load from K=0.5 to K=0.0 (1) t=0.2 msec (2) t=4 msec (3) t=8 msec

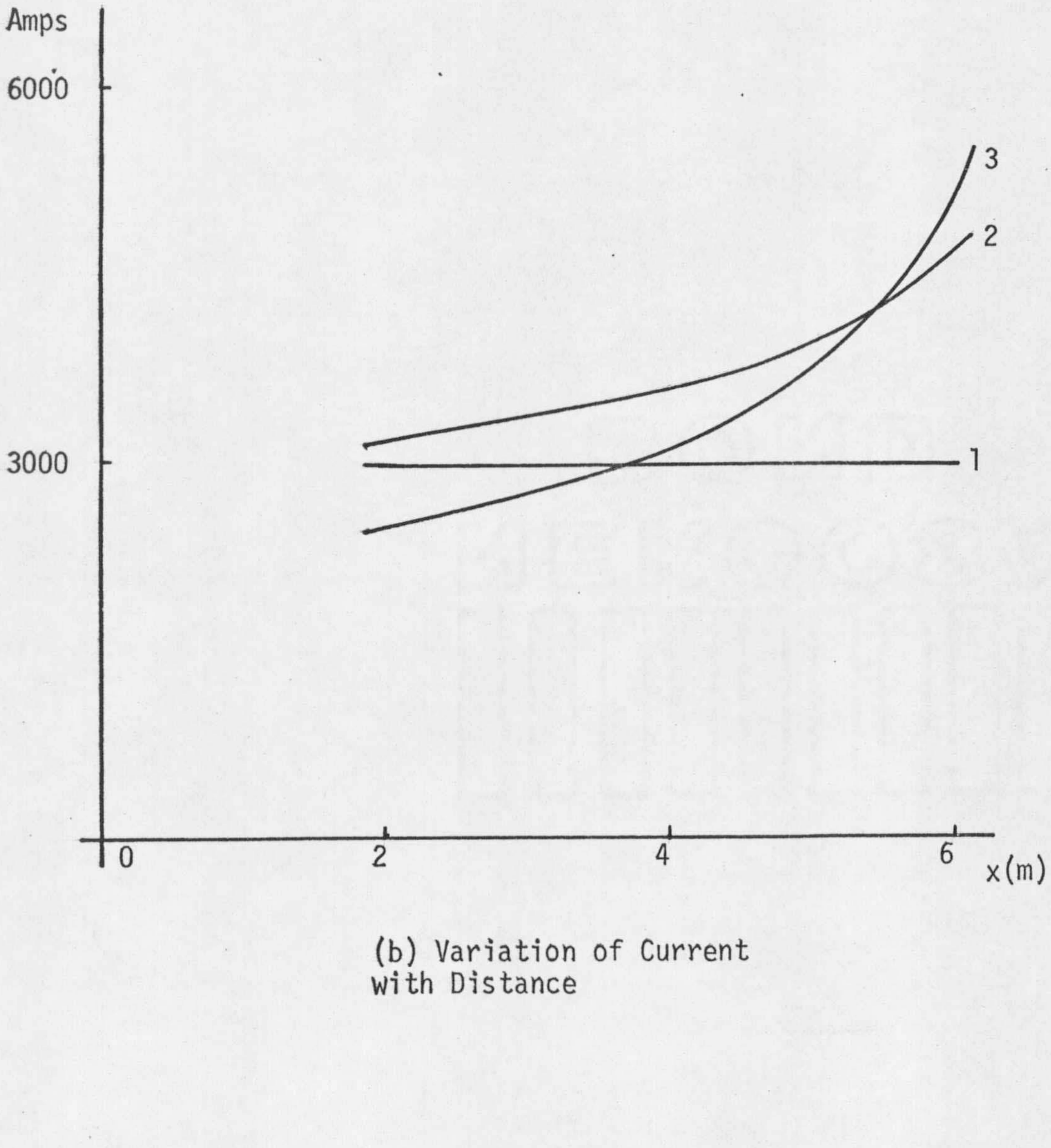

(b) Variation of Current
with Distance

Figure 4.5 (cont.)

subsonic diffuser where it will be accelerated and a shock will form. As was mentioned in Chapter III, it is the effects of this supersonic region in the diffuser, which are disastrous and which should be avoided. With the above discussion in mind, the next section will begin to develop a means by which choking can be prevented.

4.4 Choking and Generator Boundary Conditions

In the generation and distribution of electrical energy, the generating facility seldom has direct control over variations in the electrical load. For this reason, it is necessary that the generating facility be able to keep their generating equipment in an operating region which is non-destructive to the equipment, independent of load variation. For an MHD generator, this implies correcting for load variations by varying the thermodynamic boundary conditions, if possible.

To keep an MHD generator from choking after a load change which would normally cause choking, several options are available, some of which are more attractive than others. These options can be divided into three main categories. The generator can be controlled by varying the inlet, outlet or wall boundary conditions, or any combination of these quantities.

4.5 Inlet and Outlet Boundary Conditions

In order to uniquely specify inlet or outlet conditions, three states must be given. The states which are most commonly chosen are pressure (P), temperature (T), and mass flow rate (mA) and these will therefore be chosen as the three defining states. In order to prevent choking by varying the inlet or outlet conditions, mA must be decreased at the inlet and outlet while P must decrease at the inlet and increase at the outlet.

A reduction in all of these states at the inlet can be accomplished by reducing the fuel feed to the combustor, although a time lag will be introduced as the effect must propagate through the combustor and into the channel. An increase in outlet pressure can be accomplished by reducing the mass flow rate at the outlet, although this is usually not as easily accomplished as the reduction at the inlet.

4.6 Wall Boundary Conditions

Choking can also be prevented by proper variation of the wall boundary conditions, and although this method usually gives a faster response, it is also usually the most difficult to implement. There are two wall boundary conditions which are externally controllable. Wall temperature can be used to prevent choking by the addition of heat through the walls. Choking can also be prevented by a decrease in the electrical loading factor, although this violated the assumption that the load is not under the generating facility's direct control.

It therefore appears that the most easily realizable means of preventing choking, subject to the constraints presented here, is by the proper variation of the inlet parameters and possibly also the proper variation of outlet parameters. This will probably be accomplished by direct adjustment of the mass flow rate. The concern of this thesis, however, is not the development of the physical external means by which the generator parameters are varied, but rather the form of this variation. With this, and the discussion of Chapter III, in mind, the next section will begin to develop a means of preventing choking in an actual MHD generator.

4.7 Preventing Choking

In order to prevent choking in an MHD generator, it is necessary to be able to determine the effect of load changes and variations of boundary conditions on the generator, through the use of externally measurable quantities.

Two quantities which are well suited to this purpose, in that they can be measured externally and are also directly dependent on volumetric changes rather than boundary conditions, are voltage and current at each electrode pair. Using the results of Appendices A and B, the following relations can be derived for a Faraday connected generator.

$$\underline{J}\cdot\underline{E} = -\,V\cdot I/\ell\cdot h\cdot\Delta x \qquad 4.1$$

$$(\underline{J}\mathrm{x}\underline{B})_x = -\,I\cdot B/\ell\cdot\Delta x \qquad 4.2$$

It is now possible using these relations, and keeping in mind the one-dimensional assumption, to determine the internal electrical characteristics of the generator and how they are changing. In fact, based on how the voltage and current are changing, it will be possible to determine how the boundary conditions could be modified to account for load changes.

When the loading factor for an MHD generator is increased, the magnitude of the restraining force on the flow, $\underline{J}x\underline{B}_x$, is decreased and the applied pressure ratio is able to accelerate the flow. It is this effect which causes choking. In order to prevent choking, some means of adjusting the inlet and/or outlet conditions to compensate for changes in $\underline{J}x\underline{B}_x$ is necessary.

If (2.17) is studied,

$$\frac{\partial m}{\partial t} = \frac{-\partial P}{\partial x} - \frac{\partial m^2/P}{\partial x} + F + (\underline{J}x\underline{B})_x \qquad 2.17$$

it can be seen that two terms seem to be of interest, $-\frac{\partial P}{\partial x}$ and $\underline{J}x\underline{B}_x$. To prevent choking, it is necessary that any increase in $\underline{J}x\underline{B}_x$ be offset by a decrease in $-\frac{\partial P}{\partial x}$.

However, as was seen in Chapter III, it is not the pressure gradient which influences choking in a generator, but rather the pressure ratio. Because of this, (2.17), is essentially useless in calculating compensation for changes in load as it depends on the pressure gradient. There is, however, no equation which relates pressure ratio to electromagnetic effects. It is therefore necessary to develop a method based on the physical understanding of an MHD generator's response using the model of Chapter II.

Since choking is not dependent on the pressure gradient, it would seem that the critical factor in a load change might not be the magnitude of change in the $\underline{J}x\underline{B}_x$ force, but rather might be the change in the ratio of the $\underline{J}x\underline{B}_x$ force at the outlet and the $\underline{J}x\underline{B}_x$ force at the inlet of the generator. Figure 4.6, curve b, shows the variation of the ratio as a function of time for a load change from K = 0.5 to K = 0.999. Figure 4.7 shows a plot with respect to time of the ratio of the time rate of change of the momentum density at the outlet and the inlet of the generator. A comparison of Figure 4.6, curve b, and Figure 4.7, would seem to indicate that the dimensionless ratio $\underline{J}x\underline{B}_o/\underline{J}x\underline{B}_i$ is a good indicator of the "amount" of transient in the system. When the slope of this ratio is zero, the system is in steady state. Using the model of Chapter II, it is also easily shown that the form of curve b is indicative of an increase in loading factor, K.

Since this ratio can be directly calculated from terminal characteristics and generator geometry, and since it appears to be a reasonable indicator of transient response, it would seem that this ratio could be useful in determining how the pressure ratio should be adjusted to compensate for load changes.

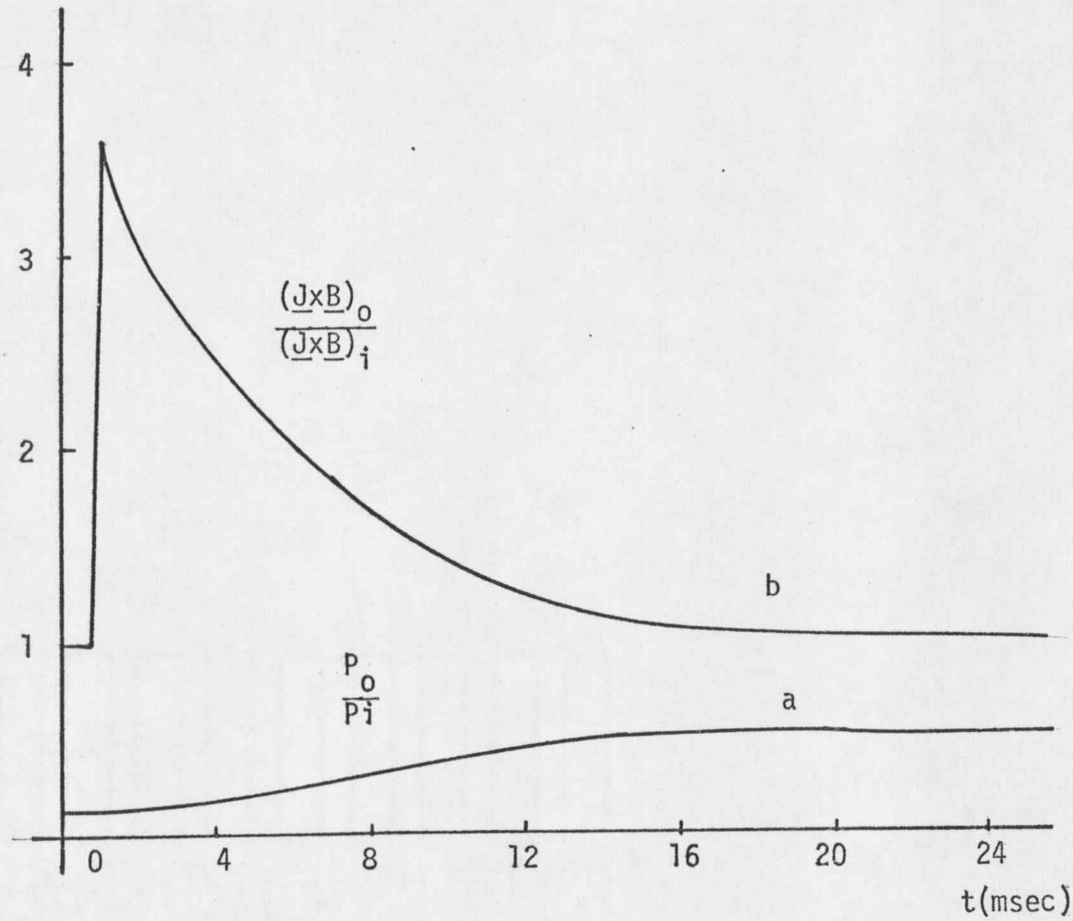

Figure 4.6 Response of Two Ratios as Load is Changed from K=0.5 to K=0.999

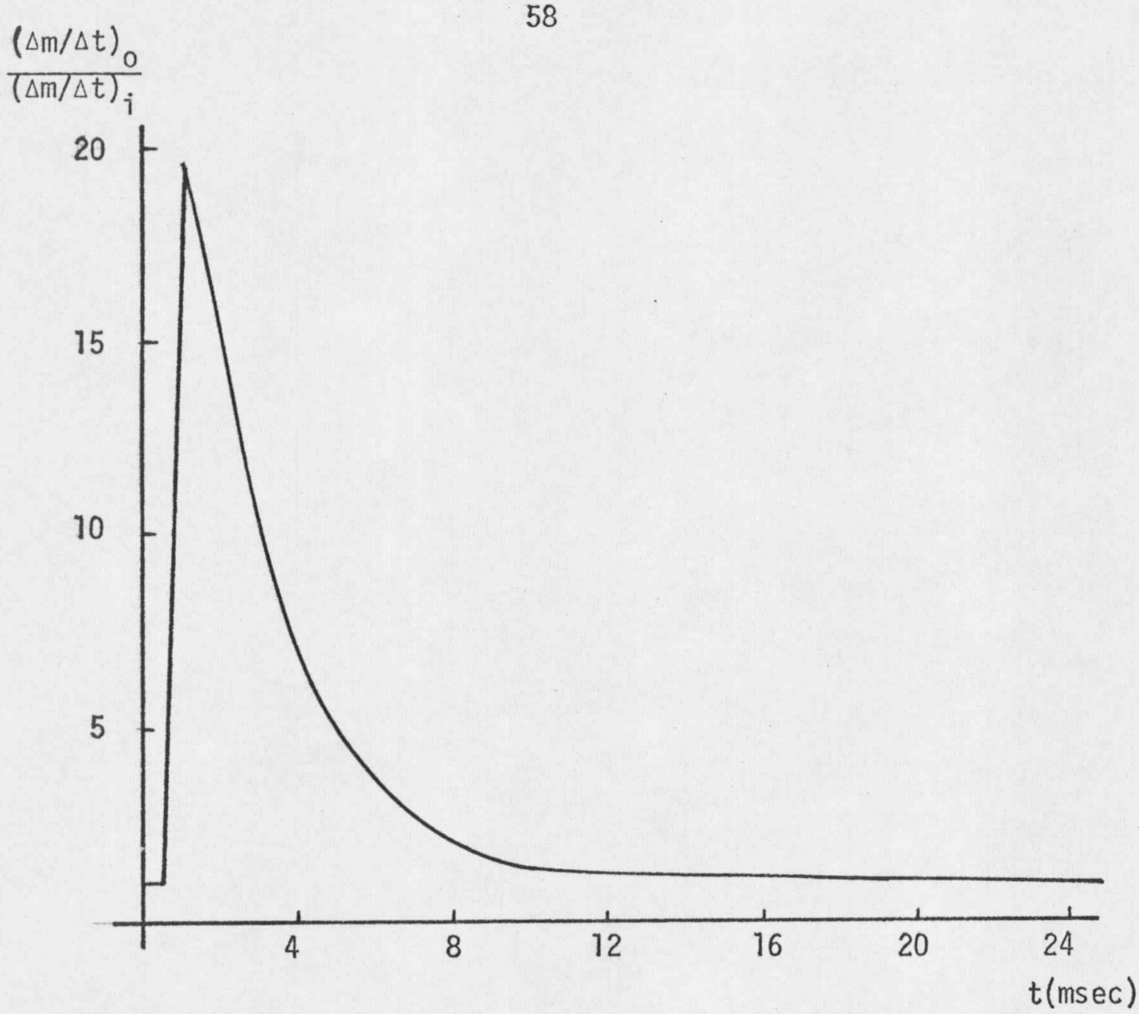

Figure 4.7 Variation of the Momentum Density Rate of Change Ratio at the Inlet and Outlet as a Function of Time

To compensate for load changes, it would seem to be necessary to adjust the pressure ratio such that the $\underline{J}x\underline{B}_x$ ratio is kept as close to unity as possible. However, it is also necessary to increase the pressure ratio such that choking will not occur. Another dimensionless ratio is therefore formed to include both these considerations, and is given by

$$JP = \frac{(\underline{J}x\underline{B})_o/(\underline{J}x\underline{B})_i}{P_o/P_i} \qquad 4.3$$

Figure 4.8 gives a plot of this ratio for the generator response of Figure 4.4.

Figure 4.9 gives the variation of this JP ratio as the outlet pressure is adjusted to compensate for the change in loading from K = 0.5 to K = 0.999. The adjustment of the outlet pressure was done by varying the mass flow rate at the outlet subject to certain constraints. The mass flow rate was not allowed to become negative or zero. When the mass flow rate was changed, it was held at its calculated value for 0.04 msec and then constrained to satisfy only the normal boundary counditions until another adjustment was necessary. An adjustment was only made if the value of JP exceeded its initial steady state value and the adjustment was then such as to return it to, as near as possible, its steady state value, subject to the above constraints. Figure 4.10 shows the Mach number distribution in the channel as this adjustment is allowed, and it is immediately obvious that the flow has not choked.

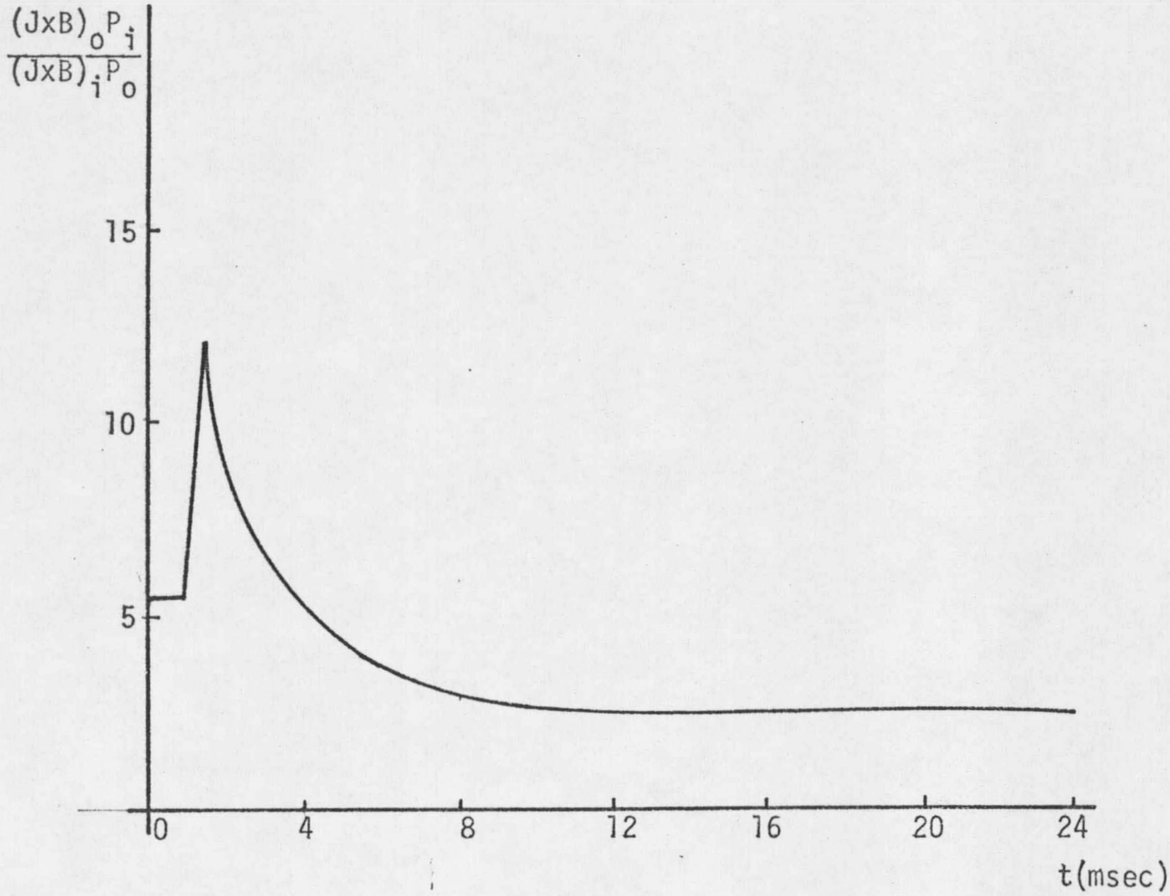

Figure 4.8 Variation of JP Ratio for a Load Change from K=0.5 to K=0.999

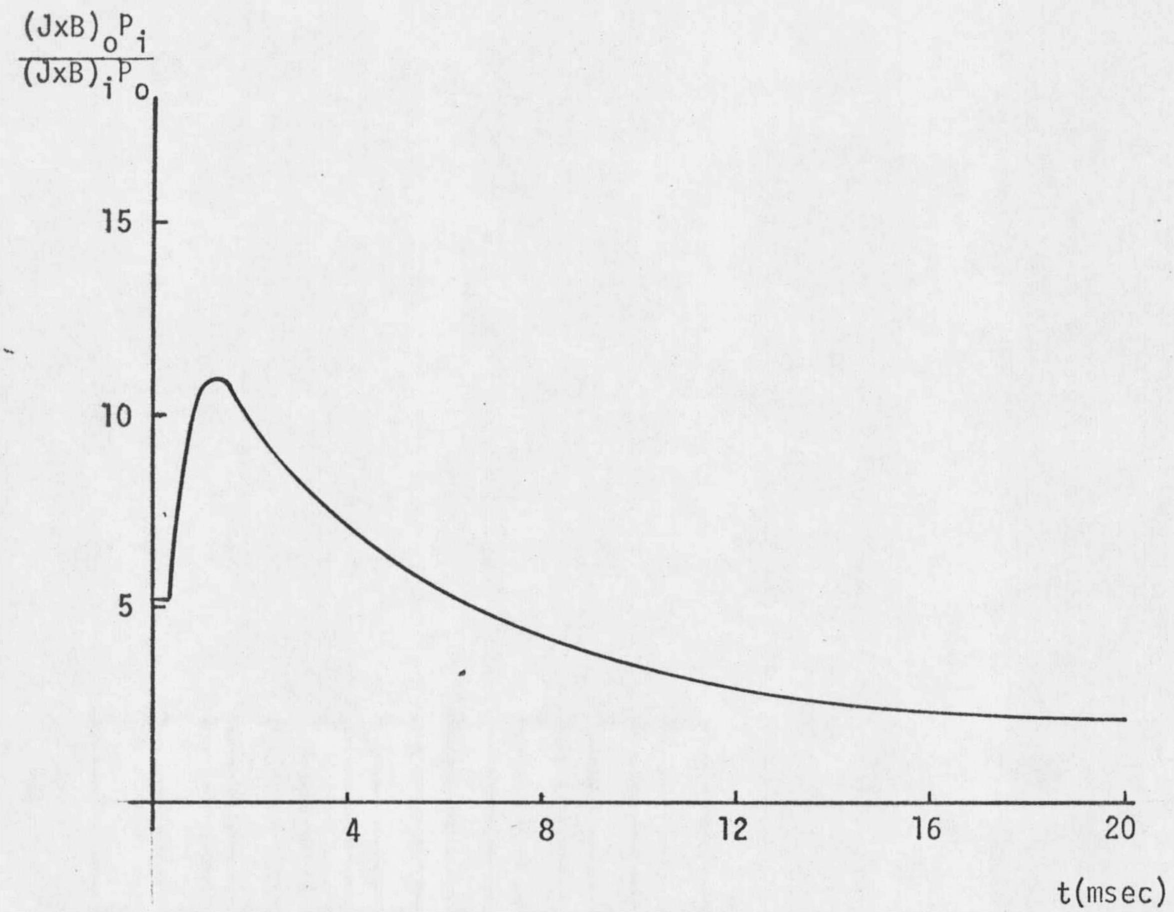

Figure 4.9 Variation of JP Ratio with Compensation as a Function of Time

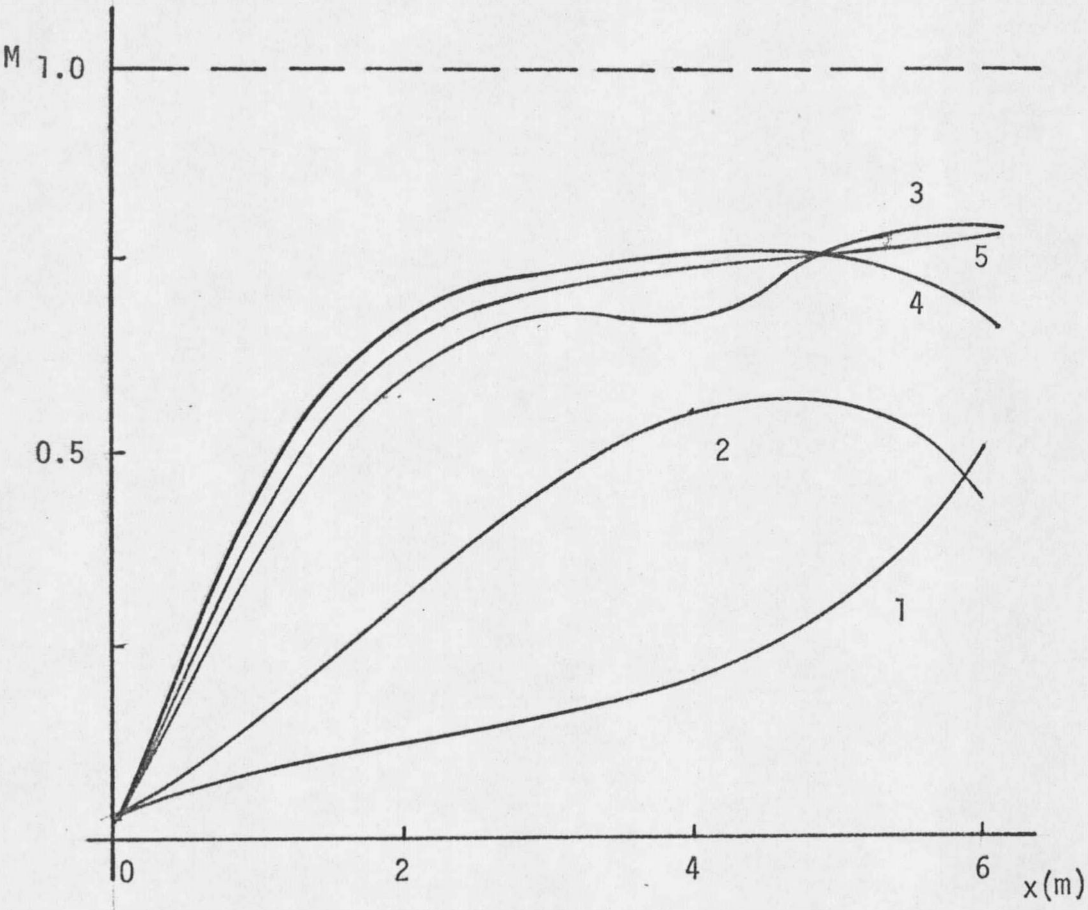

Figure 4.10 Variation of Mach Number with Distance as Compensation is Applied

The method outlined above has definitely not been an attempt to define a means of controlling a generator to prevent choking, but rather a means to show that the $\underline{J}x\underline{B}_x$ ratio is an important parameter by which the internal transients of a generator can be deduced from the terminal characteristics.

Another piece of information is also gained by a study of the $\underline{J}x\underline{B}_x$ ratio. During a transient, the point at which the $\underline{J}x\underline{B}_x$ force is greatest is the point at which choking will first occur in a constant area generator. And, although this has not been shown, a similar occurrence will probably be found in non-constant area generators. Finally, it should be noted that no means of predicting when a generator chokes has been presented.

In the next section, the results of the first four chapters will be summarized and a short section covering several areas for future research will also be presented.

CHAPTER V

5.1 Introduction

In this chapter, a summary of the results and some areas for further research which this work has indicated are presented.

5.2 Summary

The problem of choking, how it occurs, why it occurs, and what can be done to prevent it, are topics which have received little attention in the realm of MHD fluid flow. An attempt to add to the body of knowledge concerning choking has followed several steps in this thesis.

Initially, a time-dependent model of an MHD generator and nozzle was developed using numerical techniques. This model was then used to develop a familiarity with fluid flow phenomenon.

The second phase of the study involved a review of the current knowledge on steady state and transient behavior in fluid flow. During this phase, it began to become apparent that steady state and transient effects were two widely divorced areas.

The third step involved a study of the transient behavior using the model previously developed. This was done primarily to develop an understanding of fluid behavior after the flow has choked but before it has reached steady state. This was necessary and fruitful, as the transient behavior of a choked flow has been given only the slightest consideration in the past. This step also demonstrated that a familiarity with steady state effects can at times be a hinderance in th study of transient effects.

Finally, one means of determining, during a transient, where a flow is most likely to choke and what action is necessary to prevent choking, was also developed based on only the channel geometry and terminal characteristics.

These four phases have presented a very general picture of choking. This picture of choking, however, has revealed several aspects which are of interest and are therefore listed below.

The major conclusions reached by this study can now be summarized as follows.

(1) The transient behavior of a flow bears little resemblance to the behavior which is inferred for choking from the steady state equations.

(2) For the subsonic case, when a flow becomes choked, the critical point initially moves upstream and a supersonic region develops immediately downstream from the critical point. At some time after the flow chokes, the critical point will begin to move back downstream to the end of the channel and the supersonic region will be forced out of the channel.

(3) It would appear that, for a Faraday connected generator, the ratio of the x-component of the $\underline{J} \times \underline{B}$ force at the outlet of the generator and at the inlet of the generator is a good indicator of the size of the transient in a system. This would seem to occur since the

$\underline{J}x\underline{B}$ ratio appears to bear a direct relation to the ratio of the total body force, at the outlet and the inlet of the generator.

5.3 Areas for Future Research

This research has suggested the following areas for possible future research.

(1) A development of a means of numerically calculating the initial conditions for the flow based on both inlet and outlet boundary conditions rather than inlet conditions alone.

(2) A study of the means by which inlet and outlet conditions may be varied, and the determination of the time constants involved in these mechanisms.

(3) Modeling of the generator, including both nozzle and diffuser and modeling of a non-constant area duct, to determine the effect these changes will have on choking.

(4) Investigation into the validity of the one-dimensional assumption during strong transients in the flow, especially as regards electromagnetic effects.

(5) The determination of the dependency, if any, of the electrode connection scheme on the likelihood of choking.

(6) Development of a better understanding of the dependency of the terminal characteristic on the flow behavior, especially during transients.

APPENDIX A

APPROXIMATION OF THE LOADING PARAMETER, FRICTION AND HEAT TRANSFER EFFECTS AND THE MECHANICAL DISSIPATION FUNCTION

I. Loading Parameter

For a generator connected in the Faraday mode (Fig. 2.2) and configured as shown in Figure 2.1, Ohm's Law (2.7)

$$\underline{J} = \sigma(\underline{E} + \underline{V}x\underline{B}) - \mu(\underline{J}x\underline{B}) \qquad 2.7$$

can be rewritten as

$$J_x = \sigma E_x - \mu B J_y \qquad 2.7a$$

$$J_y = \sigma(E_y - uB) + \mu B J_x \qquad 2.7b$$

$$J_z = \sigma E_z \qquad 2.7c$$

where,

$$\underline{B} = B\underline{k} \qquad A.1$$

The Hall parameter is then defined as

$$\beta = \mu B \qquad A.2$$

But the Faraday connection forces the constraint,

$$J_x = 0 \qquad A.3$$

which give from (2.7b)

$$J_y = \sigma(E_y - uB) \qquad A.4$$

From Figure 2.2, we see that we can also relate J_y and E_y by

$$J_y = \frac{I_o}{\ell \cdot \Delta x} = \frac{V_o}{\ell \cdot \Delta x \cdot R_2} = \frac{-E_y \; h}{\ell \cdot \Delta x \cdot R_L} \qquad \text{A.5}$$

where all quantities are assumed constant over the electrode width Δx. Combining (A.4) and (A.5) gives,

$$\frac{-E_y \cdot h}{\ell \cdot \Delta x \cdot R_L} = \sigma(E_y - uB) \qquad \text{A.6}$$

or,

$$K = \frac{E_y}{uB} = \frac{1}{1 + \dfrac{h}{\ell \cdot \Delta x \cdot R_L \cdot \sigma}} \qquad \text{A.7}$$

where K is the well-known loading parameter. From (A.4) and (A.7), desired results are obtained.

$$(\underline{J} x \underline{B})_x = \sigma u B^2 (K-1) \qquad 2.19$$

$$\underline{J} \cdot \underline{E} = J_y E_y = \sigma (uB)^2 \; K(K-1) \qquad 2.20$$

$$K = \frac{1}{1 + \dfrac{h}{\ell \cdot \Delta x \cdot R_L \sigma}} \qquad 2.21$$

J_z and E_z are both zero since $\underline{B}$ was assumed in the z-direction only.

II. Friction and Heat Transfer

Due to the averaging of variables over the cross section in the one-dimensional model, it is necessary to develop a means to approximate the effects of the boundary layer and heat losses in the walls. We follow Sutton and Sherman in their treatment of these approximate effects. The frictional pressure drop is given by

$$F = \frac{-\tau_W C}{A} \qquad 2.22$$

where τ_W, the average shear stress at the wall is given by

$$\tau_W = 1/2 \frac{m^2}{\rho} C_f \qquad 2.23$$

and where C is the perimeter length, A is the cross sectional area, and C_f if a friction factor dependent of wall structure. We follow Heywood and Womack in their development of the friction factor

$$C_f = 0.046 \; Re^{-0.02} \qquad 2.24$$

where Re is the Reynolds number given by

$$Re = \frac{mC}{4A\eta}$$

The fluid viscosity, η, is then given by

$$\eta = 10^{-5} \sqrt{\frac{MT}{1000}} \qquad 2.25$$

where M is the Mach number and T is temperature (Rosa, 1968). The heat losses (Sutton and Sherman, 1965) are given by,

$$Q = -\frac{q_w C}{A} \qquad 2.27a$$

where

$$q_w = N_{st} mC_p \ (T - T_w) \qquad 2.27b$$

T_w is the wall temperature, and N_{st} is the local Stanton number which is typically 0.0025 (Rosa, 1968).

III. Mechanical Dissipation Function

In general, Φ represents the effects of viscosity on internal energy and is given by,

$$\Phi = \overleftrightarrow{\tau} \cdot \nabla \cdot \underline{V} = \tau_{ji} \frac{(\partial V_j)}{(\partial x_i)} \qquad A.8$$

which reduces to

$$\Phi = \tau_w = \frac{\partial m/p}{\partial x} \qquad 2.28$$

for one-dimension. τ_w is given by (2.23).

APPENDIX B

ELECTRICAL MODEL FOR A FARADAY CONNECTED MHD GENERATOR

I. The Electrical Model for a Faraday Connected Generator

Consider the circuit of Figure B.1. If a loading factor, K, is defined in the usual manner

$$K = \frac{R_L}{R_i + R_L} \qquad \text{B.1}$$

then v can be found in terms of K and v_{oc}

$$v = v_{oc}K \qquad \text{B.2}$$

and i is given by

$$i = \frac{v_{oc}K}{R_L} \qquad \text{B.3}$$

or for $R_L = 0$

$$i = v_{oc}/R_i \qquad \text{B.4}$$

Now for the loading factor developed in Appendix A for an MHD generator

$$K = \frac{E}{uB} = \frac{1}{1 + \dfrac{h}{\ell \cdot \Delta x \cdot \sigma \cdot R_L}} \qquad \text{A.7}$$

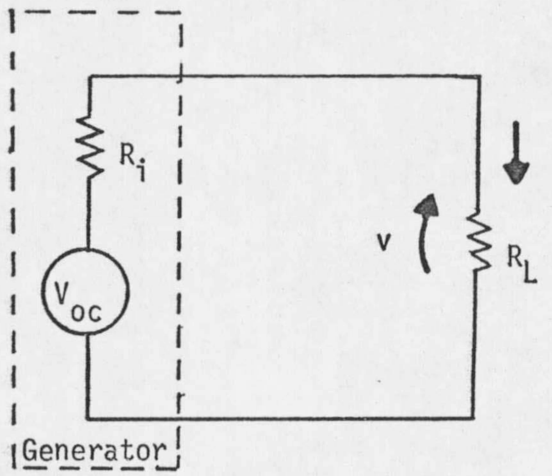

Figure B.1 Equivalent circuit for an MHD Generator with Load and internal resistance R_i can be defined

$$R_i = \frac{h}{\ell \cdot \Delta x \cdot \sigma} \qquad \text{B.5}$$

such that

$$K = \frac{1}{1 + \frac{R_i}{R_L}} = \frac{R_L}{R_i + R_L} \qquad \text{B.6}$$

From A.7 and B.2, it can then be seen that

$$v_{oc} = huB \qquad \text{B.7}$$

Based on (B.5 - B.7), it is now possible to find v and i for an MHD generator, by direct circuit concepts.

APPENDIX C

FORTRAN-IV LISTING OF MHD GENERATOR SIMULATION PROGRAM

COMMON VARIABLES

L	-	Generator Length
IH	-	Electrode Separation
IL	-	Insulator Separation
RI	-	Load Resistance at Generator inlet
DX	-	Differential x-step
GAM	-	Specific Heat Ratio
P	-	Pressure
B	-	Magnetic Flux Density
U1	-	Mass Density
U2	-	Momentum Density
U3	-	Internal Stagnation Energy
T	-	Temperature
K	-	Electrical Load Factor
CV	-	Specific Heat at Constant Volume
N	-	No. of Electrodes in Generator
R2	-	Load Resistance at L/4 from inlet
R3	-	Load Resistance at L/2 from inlet
R4	-	Load Resistance at 3L/4 from inlet
R5	-	Load resistance at Generator outlet
EJ	-	$\underline{J} \cdot \underline{E}$ at current x-step
JXB	-	$\underline{J} \times \underline{B}$ at current x-step
TAU	-	Time
R	-	Ideal Gas Constant/ Mean Molecular Weight
M	-	Mach Number
U	-	Velocity
MASS	-	Mass Flow Rate at Channel inlet
NST	-	Stanton Number
TW	-	Wall Temperature
D	-	Hydraulic Diameter
IST	-	Current step in L-W two step method

MAIN PROGRAM VARIABLES

PP - Percent of Seed in mixture
RB - Ideal Gas Constant
N1 - No. of x-steps
DT - Time-step for one step of L-W
TEND - End Time
INFLAG - 1/0; Read IC from file/Calculate IC
OUTFLAG - 1/0; Save final results/Don't save
IOUTP - No. of t-steps between output
DDT - Differential Time-step
PWR1 - Total Output Power
QT - Total Heat Losses
X - Axial Position
V - Electrode Voltage
A - Electrode Current
K1 -
K2 - Runge-Kutta Coefficents
K3 -
K4 -
K11 -
K111 -
K22 -
K222 -
K33 -
K333 -
K44 -
K444 -
DU1 -
DU2 - Final Runge-Kutta Differentials
DU3 -

```
C ****************************************************************************
C THIS PROGRAM SIMULATES THE BEHAVIOR OF A MAGNETOHYDRODYNAMIC             *
C GENERATOR CONNECTED IN THE FARADAY MODE.  THE GENERATOR IS               *
C SIMULATED BY NUMERICAL INTEGRATION OF THE COUPLED NAVIER-STOKES          *
C --MAXWELL EQUATIONS REDUCE TO A QUASI-ONE-DIMENSIONAL FORM.               *
C THIS QUASI-ON-DIMENSIONAL APPROXIMATION IS VALID IF THE                  *
C CROSS -SECTIONAL AREA IS A SLOWLY VARYING FUNCTION OF X                  *
C (I.E.  (1/A)DA/DX<<1  ).  THE SOLUTION OBTAINED IS THEN                  *
C THE AVERAGE OVER THE CROSS-SECTION OF THE FLOW PROPERTIES.               *
C ****************************************************************************
      DIMENSION U1(2,50),U2(2,50),U3(2,50),T(2,50)
      REAL L,MASS,MUO,IH,IL,NST,K,N,K1,K2,K3,K4,M,JXB
      REAL K11,K111,K22,K222,K33,K333,K44,K444
      COMMON L,IH,IL,RI,DX,GAM,P,B,U1,U2,U3,T,K,CV,N
      COMMON R2,R3,R4,R5,EJ,JXB,TAU,R,M,U,MASS,NST,TW,D,IST
C TEMPERATURE OF WALL (K)
      TW=1000.
C STAUNTON NUMBER
      READ (105,19) NST
   19 FORMAT (2F.0)
C PP PERCENT OF SEED
      PP=0.55
      PP=PP*.01
C IDEAL GAS CONSTANT M**3*ATM/MOLE*TEMP(K)
      RB=0.00008205
C CALCULATE MEAN MOLECULAR WEIGHT
C ARGON +PP% CESIUM
      MUO=(39.948*(1.-PP)+132.9054*PP)*.001
      R=RB*101325./MUO
C B IN TESLA
      READ (105,19) B
C DUCT LENGTH IN METERS
      READ (105,19) L
C INPUT ELECTRODE SEP. AND INSULATOR SEP.
      READ (105,19) IH,IL
      D=IH*IL/(IH+IL)
      READ (105,19) P
      READ (105,19) T(2,1)
      T(1,1)=T(2,1)
      READ (105,19) M
C N= NO. OF ELECTRODES
      READ (105,19) N1,N
      DX=L/N1
C TIME STEP
      READ (105,19) DT
      TAU=0.
      READ (105,19) TEND
C SPECIFIC HEAT RATIO
```

```
      READ (105,19) GAM
      CV=R/(GAM=1.)
C INPUT CONDUCTIVITY
      READ (105,19) RI
      READ (105,19) R2
      READ (105,19) R3
      READ (105,19) R4
      READ (105,19) R5
      READ (105,19) INFLAG,OUTFLAG
      READ (105,19) IOUTP
      DDT=2.*DT
      WRITE (108,50) IL,IH,L,TW,NST,DX,DDT,GAM,B,CV
   50 FORMAT ('HEIGHT(M)=',F4.2,/,'WIDTH(M)=',F4.2,/,
     #'LENGTH(M)=',F5.2,/,'WALL TEMP.(K)=',F7.1,/,'STANTON NO.='
     #,F6.4,/,'DX=',F5.4,/,'DT=',F7.6,/,'GAMMA=',F5.3,/,
     #'B(TESLA)=',F4.1,/,'CV(N*M/KG*T)=',F6.1)
      IST=2
      U1(IST,1)=U1(1,1)=P*101325./(R*T(2,1))
   52 U2(IST,1)=U2(1,1)=M*SQRT(GAM*R*T(2,1))*U1(IST,1)
      U3(IST,1)=U3(1,1)=U1(IST,1)*CV*T(2,1)+U2(IST,1)
     #*U2(IST,1)/(2.*U1(IST,1))
   15 MASS=U2(2,1)*IH*IL*4.
      K=1./(1.+IH*N/(IL*L*RL(0.0)*SIG(T(IST,1))))
      IF (RL(0.0).EQ.0.0) K=0.0
      IF (IST.EQ.2.AND.TAU.NE.0.) GO TO 30
      WRITE (108,16) TAU
   16 FORMAT (1H1,'TIME=',E10.3)
      WRITE (108,4) RI
    4 FORMAT ('RL(OHMS)=       ',F9.2)
      WRITE (108,6) K
    6 FORMAT ('K= ',F4.2)
      WRITE (108,3) MASS
    3 FORMAT ('MASS FLOW RATE(KG/S)= ',F7.2)
      WRITE (108,1)
    1 FORMAT (3X,'X(M)',2X,'(1)',1X,'RHO(KG/M**3)',1X,'(2)',
     #1X,'M(KG/M*M*S)',2X,'(3)',3X,'E(N/M*M)',3X,'(4)',3X,
     #'VEL(M/S)',/9X,'(5)',5X,'MACH',5X,'(6)',5X,'T(K)',5X,
     #'(7)',4X,'P(ATM)',4X,'(8)',5X,'SIG',/9X,'(9)',6X,'K',7X,
     #'(10)',5X,'RL',5X,'(11)',5X,'JXB',5X,'(12)',5X,'J.E',5X,
     #/8X,'(13)',6X,'V',6X,'(14)',6X,'I',6X,'(15)',6X
     #,'F',6X,'(16)',6X,'Q')
   30 PWR1=0.0
      QT=0.
      DO 10 I=1,N1+1
      IF (I.EQ.N1+1.AND.TAU.EQ.0.) GO TO 18
      X=DX*(I=1)
      IF (TAU.GT.0.) GO TO 17
      IF (X.LT.L/3.) K=V=A=EJ=JXB=0.0
```

```
      IF (INFLAG.EQ.1) GO TO 23
      CALL RNGE(K1,K11,K111,I,X,0.,0.,0.)
      CALL RNGE(K2,K22,K222,I,X+.5*DX,.5*K1,.5*K11,.5*K111)
      CALL RNGE(K3,K33,K333,I,X+.5*DX,.5*K2,.5*K22,.5*K222)
      CALL RNGE(K4,K44,K444,I,X+DX,K3,K33,K333)
      DU1=DX*(K1+2.*(K2+K3)+K4)*.16666666667
      DU2=DX*(K11+2.*(K22+K33)+K44)*.166666666667
      DU3=DX*(K111+2.*(K222+K333)+K444)*.1666666666667
   51 U1(IST,I+1)=U1(IST,I)+DU1
      U2(IST,I+1)=U2(IST,I)+DU2
      U3(IST,I+1)=U3(IST,I)+DU3
      T(IST,I+1)=(U3(IST,I+1)-U2(IST,I+1)*U2(IST,I+1)/
     #(2.*U1(IST,I+1)))/(CV*U1(IST,I+1))
      GO TO 53
   23 IF (I.GE.N1+1) GO TO 53
      IF (I.NE.1) GO TO 26
      READ (5)     U1(2,1),U2(2,1),U3(2,1)
      T(2,1)=(U3(2,1)-U2(2,1)*U2(2,1)/(2.*U1(2,1)))/
     #(CV*U1(2,1))
   26 READ (5)     U1(2,I+1),U2(2,I+1),U3(2,I+1)
      T(2,I+1)=(U3(2,I+1)-U2(2,I+1)*U2(2,I+1)/
     #(2.*U1(2,I+1)))/(CV*U1(2,I+1))
   53 K=1./(1.+IH*N/(IL*L*RL(X)*SIG(T(2,I))))
      JXB=SIG(T(2,I))*B*B*(K-1.)*U2(2,I)/U1(2,I)
      EJ=JXB*K*U2(2,I)/U1(2,I)
      A=U2(2,I)*B*IH/(U1(2,I)*(RL(X)+IH*N/(IL*L*SIG(T(2,I)))))
      V=A*RL(X)
      IF (RL(X).EQ.0.0) V=K=EJ=0.0
      IF (X.LT.L/3.) JXB=0.0
      IF (I.EQ.17) A1=A
      IF (I.EQ.N1) CALL RATIO (N1,A1,A,1)
      GO TO 18
   17 CALL TWOST(I,DT,N1)
      A=U2(2,I)*B*IH/(U1(2,I)*(RL(X)+IH*N/(IL*L*SIG(T(2,I)))))
      V=A*RL(X)
      IF (I.EQ.17) A1=A
      IF (I.EQ.N1+1.AND.IST.EQ.1) CALL RATIO (N1,A1,A,0)
   18 QT=QT+Q(I,T(2,I),U2(2,I))*DX*IH*IL
      PWR1=PWR1-V*(K-1.)*U2(2,I)*B*SIG(T(2,I))*IL*L/(N*U1(2,I))
      IF (IST.EQ.2.AND.TAU.NE.0.) GO TO 10
      IF (I.EQ.1.OR.I.EQ.16.OR.I.EQ.31.OR.I.EQ.46) GO TO 88
      IF (INT(TAU/(10.*DT)).NE.INT(TAU/(2.*DT))/5.) GO TO 10
   88 U=U2(2,I)/U1(2,I)
      P=U1(2,I)*R*T(2,I)/101325.
      M=U/SQRT(ABS(GAM*R*T(2,I)))
      WRITE (108,2) X,U1(2,I),U2(2,I),U3(2,I),U,M,T(2,I),P
     #,SIG(T(2,I)),K,RL(X),JXB,EJ,V,A,F(T(2,I),U2(2,I),U1(2,I)),
     #Q(I,T(2,I),U2(2,I))
```

```
  2 FORMAT (/,3X,F4.2,2X,'(1)',2X,1PE10.3,2X,'(2)',2X,E10.3,
   #2X,'(3)',2X,E10.3,2X,'(4)',2X,E10.3,/9X,'(5)',2X,E10.3,
   #2X,'(6)',2X,E10.3,2X,'(7)',2X,E10.3,2X,'(8)',2X,E10.3,
   #/9X,'(9)',2X,E10.3,1X,'(10)',2X,E10.3,1X,'(11)',2X,E10.3,
   #1X,'(12)',2X,E10.3,/8X,'(13)',2X,E10.3,1X,'(14)',2X,E10.3
   #,1X,'(15)',2X,E10.3,1X,'(16)',2X,E10.3)
 10 CONTINUE
    IF (IST.EQ.2.AND.TAU.NE.0.) IST=1; GO TO 15
    U1(1,N1+1)=U1(2,N1+1);U2(1,N1+1)=U2(2,N1+1);
   #U3(1,N1+1)=U3(2,N1+1);T(1,N1+1)=T(2,N1+1)
    QT=-QT*100./(MASS*(R*GAM*T(2,1)/(GAM-1.)+U2(2,1)*U2(2,1)
   #/(2.*U1(2,1)*U1(2,1))))
    WRITE (108,11) QT
 11 FORMAT (' TOTAL HEAT LOSS(%)=',F5.1)
    WRITE (108,7) PWR1
  7 FORMAT ('POWER OUTPUT(WATTS)= ',E12.5)
    WRITE (108,6) K
    IST=2
    TAU=TAU+2.*DT
    IF (TAU.LE.TEND) GO TO 15
    IF (OUTFLAG.EQ.0) GO TO 25
    DO 87 K=1,N1+1
 87 WRITE (6) U1(2,K),U2(2,K),U3(2,K)
 25 CONTINUE
    WRITE (108,20)
 20 FORMAT (1H1)
    STOP
    END
```

SUBROUTINE TWOST

ARGUMENTS

I	-	Current x-step No.
DT	-	t-step for one step of L-W
N1	-	Total No. of x-steps

VARIABLES

U12	-	U1 at outlet
U21	-	U2 at outlet
U33	-	U3 at outlet
TT	-	T at outlet
DF1	-	Differential of First Element of F(U)
DF2	-	Differential of Second Element of F(U)
DF3	-	Differential of Third Element of F(U)
UI	-	Velocity at outlet minus DX
TA	-	Average Temperature at outlet minus DX/2
U22	-	Average Momentum Density at outlet minus DX/2
U11	-	Average Mass Density at outlet minus DX/2
G1	-	First Element of G-H
G2	-	Second Element of G-H
G3	-	Third Element of G-H

```
      SUBROUTINE TWOST(I,DT,N1)
C***********************************************************************
C THIS SUBROUTINE PERFORMS THE NUMERICAL INTEGRATION OF THE TIME       *
C DEPENDENT MHD EQUATIONS.  A TWO-STEP LAX-WENDROFF METHOD IS USED     *
C WHICH IS VALID FOR SUBSONIC, SUPERSONIC, AND TRANSONIC FLOW.  THE    *
C METHOD IS ALSO ABLE TO SOLVE FOR FLOW CONDITIONS ACROSS SHOCKS.      *
C THE GENERAL EQUATION SOLVED ARE OF THE FORM,                         *
C                                                                      *
C       DU/DT=-DF(U)/DX+G                                              *
C                                                                      *
C IN THE MHD GENERATOR, AND OF THE FORM,                               *
C                                                                      *
C      DU/DT=-DF(U)/DX+G-H*DA/DX                                       *
C                                                                      *
C IN THE NOZZLE.                                                       *
C   U, F(U), G, AND H ARE ALL THREE ELEMENT VECTORS.                   *
C THIS SUBROUTINE IS DIVIDED INTO THREE SECTIONS.  SECTION ONE         *
C PERFORMS THE INTEGRATION AT THE OUTLET OF THE GENERATOR USING        *
C A BACKWARDS DIFFERENCE METHOD.  SECTION TWO PERFORMS THE SECOND      *
C STEP INTEGRATION FOR THE LAX-WENDROFF METHOD AND SECTION THREE       *
C PERFORMS THE FIRST STEP INTEGRATION FOR THE LAX WENDROFF METHOD.     *
C***********************************************************************
      DIMENSION U1(2,50),U2(2,50),U3(2,50),T(2,50)
      REAL L,MASS,MUO,IH,IL,NST,K,N,K1,K2,K3,K4,M,JXB
      COMMON L,IH,IL,RI,DX,GAM,P,B,U1,U2,U3,T,K,CV,N
      COMMON R2,R3,R4,R5,EJ,JXB,TAU,R,M,U,MASS,NST,TW,D,IST
      U=U2(IST,I)/U1(IST,I)
      X=DX*(I-1)
      IF (IST.EQ.2) GO TO 15
      IF (I.NE.N1+1.AND.I.NE.1) GO TO 20
      IF (I.EQ.1) JXB=EJ=K=V=A=0.0;RETURN
C***********************************************************************
C       SECTION ONE                                                    *
C                                                                      *
C                                                                      *
C THIS SECTION PERFORMS THE NUMERICAL INTEGRATION OF THE TIME-         *
C DEPENDENT MHD EQUATIONS AT THE OUTLET OF THE GENERATOR USING         *
C A BACKWARDS DIFFERENCE METHOD.                                       *
C **********************************************************************
      U12=U1(2,N1+1);U21=U2(2,N1+1);U33=U3(2,N1+1);TT=T(2,N1+1)
  999 J=N1;J1=N1+1
      DF1=U2(2,J1)-U2(2,J)
      DF2=(GAM-1.)*(U3(2,J1)-U3(2,J))+(1.5-.5*GAM)*(U2(2,J1)
     #*U2(2,J1)/U1(2,J1)-U2(2,J)*U2(2,J)/U1(2,J))
      DF3=GAM*(U2(2,J1)*U3(2,J1)/U1(2,J1)-U2(2,J)
     #*U3(2,J)/U1(2,J))-(GAM-1.)*.5*(U2(2,J1)*U2(2,J1)
     #*U2(2,J1)/(U1(2,J1)*U1(2,J1))-U2(2,J)*U2(2,J)
     #*U2(2,J)/(U1(2,J)*U1(2,J)))
      UI=U2(2,J)/U1(2,J)
```

```
      U=U2(2,J1)/U1(2,J1)
      M=U/SQRT(ABS(GAM*R*T(2,I)))
      TA=(T(2,J)+T(2,J1))*.5
      K=1./(1.+IH*N/(IL*L*RL(J*DX)*SIG(TA)))
      IF (RL(J*DX).EQ.0.0) K=0.0
      JXB=.5*SIG(TA)*B*B*(K-1.)*(UI+U)
      EJ=JXB*.5*(UI+U)*K
      U22=.5*(U2(2,I)+U2(2,I-1))
      U11=.5*(U1(2,I)+U1(2,I-1))
      G2=F(TA,U22,U11)+JXB
      G3=EJ+Q(I,TA,U22)
      A=U2(2,I)*B*IH/(U1(2,I)*(RL(J1*DX)+IH*N/(IL*L*SIG(TA))))
      U1(2,I)=U1(2,I)-2.*DT*(DF1/DX)
      U2(2,I)=U2(2,I)-2.*DT*(DF2/DX-G2)
      A1=U2(2,I)*B*IH/(U1(2,I)*(RL(J1*DX)+IH*N/(IL*L*SIG(TA))))
      IF (M.GE.1.00) U3(2,I)=U3(2,I)-2.*DT*(DF3/DX-G3)
      T(2,I)=(U3(2,I)-U2(2,I)*U2(2,I)/(2.*U1(2,I)))
     #/(CV*U1(2,I))
      RETURN
C ***********************************************************************
C     SECTION TWO                                                       *
C                                                                       *
C                                                                       *
C THIS SECTION PERFORMS THE NUMERICAL INTEGRATION OF THE TIME-          *
C DEPENDENT MHD EQUATIONS FOR THE SECOND STEP OF THE LAX-WENDROFF       *
C METHOD.                                                               *
C***********************************************************************
   20 DF1=U2(IST,I)-U2(IST,I-1)
      DF2=(GAM-1.)*(U3(IST,I)-U3(IST,I-1))+(1.5-.5*GAM)*(U2(IST,I)
     #*U2(IST,I)/U1(IST,I)-U2(IST,I-1)*U2(IST,I-1)/U1(IST,I-1))
      DF3=GAM*(U2(IST,I)*U3(IST,I)/U1(IST,I)-U2(IST,I-1)
     #*U3(IST,I-1)/U1(IST,I-1))-(GAM-1.)*.5*(U2(IST,I)*U2(IST,I)
     #*U2(IST,I)/(U1(IST,I)*U1(IST,I))-U2(IST,I-1)*U2(IST,I-1)
     #*U2(IST,I-1)/(U1(IST,I-1)*U1(IST,I-1)))
      UI=U2(IST,I-1)/U1(IST,I-1)
      TA=(T(IST,I)+T(IST,I-1))*.5
      IF (X.LE.L/3.) K=JXB=EJ=0.0;     GO TO 21
      K=1./(1.+IH*N/(IL*L*RL(X)*SIG(TA)))
      IF (RL(X).EQ.0.0) K=0.0
      JXB=.5*SIG(TA)*B*B*(K-1.)*(UI+U)
      EJ=.5*JXB*K*(U+UI)
   21 G1=-.5*(U2(IST,I)+U2(IST,I-1))*.5*(DA(X-.5*DX)+DA(X+.5*DX))
      U22=.5*(U2(IST,I)+U2(IST,I-1))
      U11=.5*(U1(IST,I)+U1(IST,I-1))
      G2=F(TA,U22,U11)+JXB+.5*(U+UI)*G1
      G3=EJ+Q(I,TA,U22)+G1*(GAM*(U3(IST,I)+U3(IST,I-1))/(U1(IST,I)+U1
     #(IST,I-1))-(GAM-1.)*.25*(U+UI)*(U+UI)/2.)
      U1(2,I)=U1(2,I)-2.*DT*(DF1/DX-G1)
      U2(2,I)=U2(2,I)-2.*DT*(DF2/DX-G2)
```

```
      U3(2,I)=U3(2,I)-2.*DT*(DF3/DX-G3)
      T(2,I)=(U3(2,I)-U2(2,I)*U2(2,I)/(2.*U1(2,I)))
     #/(CV*U1(2,I))
      RETURN
C ********************************************************************
C     SECTION THREE                                                  *
C                                                                    *
C THIS SECTION PERFORMS THE NUMERICAL INTEGRATION OF THE TIME-       *
C DEPENDENT MHD EQUATIONS FOR THE FIRST STEP OF THE LAX-WENDROFF     *
C METHOD.                                                            *
C ********************************************************************
   15 IF (I.EQ.N1+1) RETURN
      DF1=U2(IST,I+1)-U2(IST,I)
      DF2=(GAM-1.)*(U3(IST,I+1)-U3(IST,I))+(1.5-.5*GAM)*(U2(IST,I+1)
     #*U2(IST,I+1)/U1(IST,I+1)-U2(IST,I)*U2(IST,I)/U1(IST,I))
      DF3=GAM*(U2(IST,I+1)*U3(IST,I+1)/U1(IST,I+1)-U2(IST,I)
     #*U3(IST,I)/U1(IST,I))-(GAM-1.)*.5*(U2(IST,I+1)*U2(IST,I+1)
     #*U2(IST,I+1)/(U1(IST,I+1)*U1(IST,I+1))-U2(IST,I)*U2(IST,I)
     #*U2(IST,I)/(U1(IST,I)*U1(IST,I)))
      UI=U2(IST,I+1)/U1(IST,I+1)
      TA=(T(IST,I)+T(IST,I+1))*.5
      IF (X+.5*DX.LE.L/3.) K=JXB=EJ=0.0; GO TO 16
      K=1./(1.+IH*N/(IL*L*RL(X+.5*DX)*SIG(TA)))
      IF (RL(X+.5*DX).EQ.0.0) K=0.0
      JXB=.5*SIG(TA)*B*B*(K-1.)*(UI+U)
      EJ=.5*JXB*K*(U+UI)
   16 G1=-.5*(U2(IST,I)+U2(IST,I+1))*.5*(DA(X)+DA(X+DX))
      U22=.5*(U2(IST,I)+U2(IST,I+1))
      U11=.5*(U1(IST,I)+U1(IST,I+1))
      G2=F(TA,U22,U11)+JXB+.5*(U+UI)*G1
      G3=EJ+Q(I,TA,U22)+G1*(GAM*(U3(IST,I)+U3(IST,I+1))/(U1(IST,I)+
     #U1(IST,I+1))-(GAM-1.)*.25*(UI+U)*(UI*U)/2.)
      U1(1,I)=.5*(U1(2,I+1)+U1(2,I))-DT*(DF1/DX-G1)
      U2(1,I)=.5*(U2(2,I+1)+U2(2,I))-DT*(DF2/DX-G2)
      U3(1,I)=.5*(U3(2,I+1)+U3(2,I))-DT*(DF3/DX-G3)
      T(1,I)=(U3(1,I)-U2(1,I)*U2(1,I)/(2.*U1(1,I)))/(CV
     #*U1(1,I))
      RETURN
      END
```

FUNCTION SIG

ARGUMENT

TT - Temperature at Point of Interest

VARIABLES

TLOC - Adjusted Temperature
SIG - Conductivity

```
      FUNCTION SIG(TT)
C ***********************************************************************
C THIS SUBROUTINE CALCULATES THE CONDUCTIVITY OF THE WORKING FLUID     *
C IN THE GENERATOR. THE WORKING FLUID IS ARGON + 0.55% CESIUM AND      *
C THE CONDUCTIVITY IS ASSUMED TO BE A FUNCTION OF THE GAS              *
C TEMPERATURE ONLY.  THE CALCULATION IS BASED ON A GRAPH GIVEN IN      *
C ROSA (1964).                                                         *
C ***********************************************************************
      DIMENSION U1(2,50),U2(2,50),U3(2,50),T(2,50)
      REAL L,MASS,MUO,IH,IL,NST,K,N,K1,K2,K3,K4,M,JXB
      COMMON L,IH,IL,RI,DX,GAM,P,B,U1,U2,U3,T,K,CV,N
      COMMON R2,R3,R4,R5,EJ,JXB,TAU,R,M,U,MASS,NST,TW,D,IST
      TLOC=(TT/1500.)+.333333333
      IF (TLOC.GT.50.) TLOC=50.
      SIG=10.**TLOC
      RETURN
      END
```

FUNCTION RL

ARGUMENT

X - Axial Position

VARIABLES

Y - Adjusted x Position
RL - Load Resistance

```
      FUNCTION RL(X)
C *****************************************************************
C THIS SUBROUTINE CALCULATES THE RESISTANCE AT EACH ELECTRODE PAIR  *
C IN A FARADAY CONNECTED GENERATOR.  THIS RESISTANCE IS FIGURED     *
C USING A CURVE FIT OF FIVE NOMINAL VALUES OF RESISTANCE.  THESE    *
C FIVE VALUES ARE INPUT AS INITIAL DATA AND ARE ASSUMED TO BE       *
C EQUALLY SPACED DOWN THE CHANNEL.                                  *
C *****************************************************************
      DIMENSION U1(2,50),U2(2,50),U3(2,50),T(2,50)
      REAL L,MASS,MUO,IH,IL,NST,K,N,K1,K2,K3,K4,M,JXB
      COMMON L,IH,IL,RI,DX,GAM,P,B,U1,U2,U3,T,K,CV,N
      COMMON R2,R3,R4,R5,EJ,JXB,TAU,R,M,U,MASS,NST,TW,D,IST
      Y=4.*(X-L/3.)/L
      IF (X.LE.L/3.) RL=0.;RETURN
      IF (TAU.LT.0.00020)RL=1./(SIG(T(IST,INT(1+X/DX)))*L/N);RETURN
      RL=RI+Y*(R2-RI)+Y*(Y-1.)*(R3-2.*R2+RI)*.5+Y*(Y-1.)*(Y-2.)*
     #(R4-3.*R3+3.*R2-RI)*.166666667+Y*(Y-1.)*(Y-2.)*(Y-3.)*
     #(R5-4.*R4+6.*R3-4.*R2+RI)*.041666667
      RETURN
      END
```

SUBROUTINE RNGE

ARGUMENTS

DK1	-	Runge-Kutta Coefficients
DK2	-	
DK3	-	
DK4	-	
DK5	-	
DK6	-	
I	-	Current x-step No.
XX	-	Axial Position

VARIABLES

U11	-	U1 plus Runge-Kutta Differential
U22	-	U2 plus Runge-Kutta Differential
U33	-	U3 plus Runge-Kutta Differential
TT	-	Temperature
DENOM	-	Common Denominator
DU1	-	Runge-Kutta Differentials
DU2	-	
DU3	-	

```
      SUBROUTINE RNGE(DK1,DK2,DK3,I,XX,DK4,DK5,DK6)
C *****************************************************************
C THIS SUBROUTINE PERFORMS THE NUMERICAL INTEGRATION OF THE STEADY  *
C STATE MHD EQUATIONS TO DETERMINE A SET OF INITIAL CONDITIONS FROM *
C WHICH THE TIME-DEPENDENT SOLUTION CAN BE DETERMINED.  THIS IS     *
C DONE USING A FOURTH ORDER RUNGE-KUTTA INTEGRATION SCHEME.         *
C *****************************************************************
      DIMENSION U1(2,50),U2(2,50),U3(2,50),T(2,50)
      REAL L,MASS,MUO,IH,IL,NST,K,N,K1,K2,K3,K4,M,JXB
      COMMON L,IH,IL,RI,DX,GAM,P,B,U1,U2,U3,T,K,CV,N
      COMMON R2,R3,R4,R5,EJ,JXB,TAU,R,M,U,MASS,NST,TW,D,IST
      U11=U1(IST,I)+DX*DK4
      U22=U2(IST,I)+DX*DK5
      U33=U3(IST,I)+DX*DK6
      TT=(U33-U22*U22/(2.*U11))/(CV*U11)
      K=1./(1.+IH*N/(IL*L*RL(XX)*SIG(TT)))
      JXB=SIG(TT)*B*B*(K-1.)*U22/U11
      EJ=JXB*K*U22/U11
      IF (RL(XX).EQ.0.0) EJ=K=V=0.0
      IF (XX.LT.L/3.) JXB=0.0
      DENOM=-U22*U22*(GAM-1.)*GAM/(2.*U11)+(GAM-1.)*GAM*U33
     1-U22*U22/U11
      UI=U22/U11
      DK1=((F(T(IST,I),U22,U11)+JXB)*(U22*GAM/U11)-(Q(I,TT,U22)+EJ)*
     1(GAM-1.))/(U22*DENOM/(U11*U11))
      DK3=((-U22*(3.-GAM)/2.)*(Q(I,TT,U22)+EJ)-((GAM-1.)*U22*U22/U11
     1-GAM*U33)*(F(T(IST,I),U22,U11)+JXB))/DENOM
      DK2=0.
   10 DENOM=DENOM*U22/(U11*U11)
      DU1=U22**3*DA(XX)/(U11*U11*DENOM)
      DK2=DK2-U22*DA(XX)
      DK3=DK3-DU1*(U22*U22*(-GAM*GAM+2.*GAM-1)/(2.*U11)+(GAM-2)*GAM
     1*U33)/U11
      DK1=DK1+DU1
      RETURN
      END
```

FUNCTION Q

ARGUMENTS

I	-	Current x-step No.
TT	-	Temperature at Point of Interest
U22	-	Momentum Density at Point of Interest

VARIABLE

Q	-	Heat Losses for Current Differential Volume

```
      FUNCTION Q(I,TT,U22)
C ***********************************************************************
C THIS SUBROUTINE CALCULATES THE HEAT LOSSES FOR A DIFFERENTIAL         *
C VOLUME OF CHANNEL                                                     *
C***********************************************************************
      DIMENSION U1(2,50),U2(2,50),U3(2,50),T(2,50)
      REAL L,MASS,MU0,IH,IL,NST,K,N,K1,K2,K3,K4,M,JXB
      COMMON L,IH,IL,RI,DX,GAM,P,B,U1,U2,U3,T,K,CV,N
      COMMON R2,R3,R4,R5,EJ,JXB,TAU,R,M,U,MASS,NST,TW,D,TST
      IF (DX*(I-1).LT.L/3.) Q=0.0 ;RETURN
      Q=-NST*U22*GAM*R*(TT-TW)*4.0/((GAM-1.)*D)
      RETURN
      END
```

FUNCTION F

ARGUMENTS

TT	-	Temperature at Point of Interest
U22	-	Momentum Density at Point of Interest
U11	-	Mass Density at Point of Interest

VARIABLES

UI	-	Velocity
VIS	-	Viscosity
RE	-	Reynolds Number
F	-	Friction Losses for Differential Volume

```
      FUNCTION F(TT,U22,U11)
C*********************************************************************
C THIS SUBROUTINE CALCULATES THE LOSSES DUE TO FRICTION FOR A        *
C DIFFERENTIAL VOLUME IN THE MHD GENERATOR.                          *
C ********************************************************************
      DIMENSION U1(2,50),U2(2,50),U3(2,50),T(2,50)
      REAL L,MASS,MUO,IH,IL,NST,K,N,K1,K2,K3,K4,M,JXB
      COMMON L,IH,IL,RI,DX,GAM,P,B,U1,U2,U3,T,K,CV,N
      COMMON R2,R3,R4,R5,EJ,JXB,TAU,R,M,U,MASS,NST,TW,D,IST
      UI=U22/U11
      VIS=.00001*SQRT(ABS(UI*SQRT(ABS(TT/(GAM*R)))/1000.))
      RE=ABS(U22*D/VIS)
      F=-U22*U22*0.092/((RE**0.2)*D*U11)
      RETURN
      END
```

FUNCTION DA

ARGUMENT

X - Axial Position

VARIABLES

XLL - Position of Nozzle-Generator Interface
XH - Electrode Walls Separation
XL - Insulator Walls Separation
DA - Rate of Change of Area with x

```
      FUNCTION DA(X)
C *****************************************************************************
C THIS SBROUTINE CALCULATES THE RATE OF CHANGE OF THE AREA IN                 *
C THE NOZZLE FOR EACH X-STEP.                                                 *
C *****************************************************************************
      DIMENSION U1(2,50),U2(2,50),U3(2,50),T(2,50)
      REAL L,MASS,MUO,IH,IL,NST,K,N,K1,K2,K3,K4,M,JXB
      COMMON L,IH,IL,RI,DX,GAM,P,B,U1,U2,U3,T,K,CV,N
      COMMON R2,R3,R4,R5,EJ,JXB,TAU,R,M,U,MASS,NST,TW,D,IST
      XLL=L/3.-DX
      IF (X.GT.XLL)  DA=0.0;RETURN
      XH=-IH*X/XLL+2.*IH
      XL=-IL*X/XLL+2.*IL
      IF (XL.LT.IL.OR.XH.LT.IH) XH=IH;XL=IL
      DA=-((IL/XLL)*XH+(IH/XLL)*XL)/(XH*XL)
      RETURN
      END
```

SUBROUTINE RATIO

ARGUMENTS

N1	-	No. of Electrodes
A1	-	Current at Generator Inlet
A2	-	Current at Generator Outlet
IFF	-	Flag

VARIABLES

J	-	No. of x-steps
DIF	-	Difference between actual and required value of RAT
RAT	-	JP Ratio
FINT	-	Intermediate Value

```
      SUBROUTINE RATIO (N1,A1,A2,IFF)
C ***********************************************************************
C THIS SUBROUTINE CALCULATES THE REQUIRED CHANGE IN OUTLET PRESSURE *
C SUCH THAT THE CHANGE IN THE JxB RATIO (OUTLET TO INLET) IS         *
C COMPENSATED FOR AND CHOKING WILL NOT OCCUR.                         *
C ***********************************************************************
      DIMENSION U1(2,50),U2(2,50),U3(2,50),T(2,50)
      REAL L,MASS,MUO,IH,IL,NST,K,N,K1,K2,K3,K4,M,JXB
      COMMON L,IH,IL,RI,DX,GAM,P,B,U1,U2,U3,T,K,CV,N
      COMMON R2,R3,R4,R5,EJ,JXB,TAU,R,M,U,MASS,NST,TW,D,IST
      IF (IFF.EQ.1) GO TO 10
      J=N1+1
      DIF=RAT*(A2/A1)*(U1(2,1)*T(2,1)/(U1(2,J)*T(2,J)))
    5 IF (DIF.LE.1.00) RETURN
      FINT=(1-DIF)*U1(2,J)*R*T(2,J)+(GAM-1.)*U2(2,J)*U2(2,J)
     #/(2.*U1(2,J))
      IF (FINT.LE.0.0) DIF=DIF*0.8;GO TO 5
      U2(2,J)=SQRT(2.*FINT*U1(2,J)/(GAM-1.))
      RETURN
   10 RAT=A1*U1(2,N1+1)*T(2,N1+1)/(A2*U1(2,1)*T(2,1))
      RETURN
      END
```

APPENDIX D

FORTRAN-IV LISTING OF PROGRAM TO DETERMINE THE CRITICAL POINT

COMMON VARIABLES

M	-	Mach No.
K	-	Loading Factor
U1	-	Mass Density
U2	-	Momentum Density
U3	-	Stagnation Energy
GAM	-	Specific Heat Ratio
CV	-	Specific Heat at Constant Volume
R	-	Ideal Gas Constant
B	-	Magnetic Flux Density
DX	-	Differential x-step

MAIN PROGRAM VARIABLES

P1	-	Pressure at Generator Inlet
T	-	Temperature at Generator Inlet
M1	-	Mach No. at Generator Inlet
PO	-	Stagnation Pressure at Nozzle Inlet
P	-	Outlet Pressure
PC	-	Critical Pressure
X	-	Axial Position
RP	-	Critical Pressure Ratio

```
C*********************************************************************
C THIS PROGRAM PERFORMS THE NUMERICAL INTEGRATION OF THE STEADY      *
C STATE MHD EQUATIONS TO DETERMINE THE CONDITIONS AT WHICH           *
C CHOKING WILL OCCUR.  THE EQUATIONS ARE INTEGRATED, FOR VARIOUS     *
C VALUES OF LOADING, USING A FOURTH ORDER RUNGE-KUTTA METHOD         *
C UNTIL THE CRITICAL POINT IS REACHED.  THE CRITICAL PRESSURE        *
C RATIO, CRITICAL PRESSURE, AND LENGTH OF THE GENERATOR ARE          *
C THEN OUTPUT.                                                       *
C ********************************************************************
      REAL M,K,M1
      COMMON M,K,U1,U2,U3,GAM,CV,R,B,DX
    1 FORMAT (2F.0)
      READ (105,1) P1
      READ (105,1) T
      READ (105,1) M1
      READ (105,1) P0
      READ (105,1) DX
      READ (105,1) B
      GAM=5./3.
      R=186.4235
      CV=R/(GAM-1.)
      WRITE (108,2)
    2 FORMAT (1H1,10X,'K',10X,'RP',10X,'P',12X,'M',12X,'P*',12X,'X')
      DO 100 K=0.,.91,.1
      U1=P1*101325/(R*T)
      U2=M1*SQRT(GAM*R*T)*U1
      U3=U1*CV*T+U2*U2/(2.*U1)
      I=1
   97 CALL RNGE
      M=U2/(U1*SQRT(ABS(GAM*R*(U3-U2*U2/(2.*U1))/(U1*CV))))
      IF (M.GE..98) GO TO 99
      I=I+1
      GO TO 97
   99 P=(GAM-1.)*(U3-U2*U2/(2.*U1))/101325.
      PC=P*(SQRT((2+.666666667*M*M)/2.666666667))**5
      X=DX*(I-1)
      RP=PC/P0
      WRITE (108,3) K,RP,P,M,PC,X
    3 FORMAT (1X,6(1PE10.3,4X))
  100 CONTINUE
      STOP
      END
```

SUBROUTINE RNGE VARIABLES

K1 -	Runge-Kutta Coefficients
K3 -	
U11 -	Intermediate Value of U1
U33 -	Intermediate Value of U3
TC -	Adjusted Temperature for Conductivity Calculation
JXB -	$\underline{J \mathrm{x} B}$
EJ -	$\bar{J}\cdot\bar{E}$
DENOM -	Common Denominator

```
      SUBROUTINE RNGE
C ***********************************************************************
C THIS SUBROUTINE IS USED TO PERFORM THE RUNGE-KUTTA INTEGRATION       *
C OF THE STEADY STATE MHD EQUATIONS.                                   *
C ***********************************************************************
      REAL M,K,K1(5),K3(5),JXB
      COMMON M,K,U1,U2,U3,GAM,CV,R,B,DX
      K1(1)=0.0
      K3(1)=0.0
      DO 10 I=1,4
      U11=U1+DX*K1(I)
      U33=U3+DX*K3(I)
      T=(U33-U2*U2/(2.*U11))/(CV*U11)
      TC=(T/1500.)+.3333333333
      JXB=(10.**TC)*B*B*(K-1.)*U2/U11
      EJ=JXB*K*U2/U11
      DENOM=-U2*U2*(GAM-1.)*GAM/(2.*U11)+(GAM-1.)*GAM*U33-U2*U2/U11
      K1(I)=(JXB*(U2*GAM/U11)-EJ*(GAM-1.))/(U2*DENOM/(U11*U11))
      K3(I)=((-U2*(3.-GAM)/2.)*EJ-((GAM-1.)*U2*U2/U11-GAM*U33)*JXB)/
     #DENOM
      K1(I+1)=.5*K1(I)
      K3(I+1)=.5*K3(I)
      IF (I.EQ.3) K1(I+1)=K1(I);K3(I+1)=K3(I)
   10 CONTINUE
      U1=U1+DX*(K1(1)+2.*(K1(2)+K1(3))+K1(4))*.1666666667
      U3=U3+DX*(K3(1)+2.*(K3(2)+K3(3))+K3(4))*.1666666667
      IF (U1.LT.0.0.OR.U3.LT.0.0) STOP
      RETURN
      END
```

REFERENCES

Chapman, A. and Walker, W., Introductory Gas Dynamics, Holt, Rinehart and Winston, Inc., N.Y., 1971.

Feynman, R., The Feynman Lectures on Physics, Vol. I, Addison-Wesley Publishing Company, Reading, Mass., 1963, pp. 40-7--40-8.

Gerald, C., Applied Numerical Analysis, Addison-Wesley Publishing Company, Reading, Mass., 1970, pp. 118-119.

Heywood, J. and Womack, G., ed., Open-Cycle MHD Power Generation, Pergamon Press, Oxford, 1969.

Hughes, W.F. and Young, F.J., The Electromagnetodynamics of Fluids, John Wiley and Sons, Inc., N.Y., 1966.

Pai, S.I., Magnetogasdynamics, Prentice-Hall, Inc., Englewood Cliffs, N.J., 1962.

Roache, P.J., Computational Fluid Dynamics, Hermosa Press, 1972.

Rosa, R.J., Magnetohydrodynamic Energy Conversion, McGraw-Hill Book Co., N.Y., 1968.

Shapiro, A., The Dynamics and Thermodynamics of Compressible Fluid Flow, Vol. 1, Ronald Press Co., N.Y., 1953.

Sutton, G.W. and Sherman, A., Engineering Magnetohydrodynamics, McGraw-Hill Book Co., N.Y., 1965.

Turabin, K.L., A Manual for Writers of Term Papers, Thesis, and Dissertations, 3rd ed., Chicago, University of Chicago Press, 1967.